Bioorganic & Medicinal Chemistry 18 (2010) 1213–1226

Contents lists available at ScienceDirect

Bioorganic & Medicinal Chemistry

journal homepage: www.elsevier.com/locate/bmc

Synthesis and the biological evaluation of arylnaphthalene lignans as anti-hepatitis B virus agents

Damodar Janmanchi [a,b,†], Ya Ping Tseng [a,†], Kuei-Chen Wang [a], Ray Ling Huang [c], Chih Hsiu Lin [b,*], Sheau Farn Yeh [a,*]

[a] Institute of Biochemistry and Molecular Biology, National Yang-Ming University, Taipei, Taiwan, ROC
[b] Institute of Chemistry, Academia Sinica, Taipei, Taiwan, ROC
[c] Department of Biological Science and Technology, Meiho Institute of Technology, Pingtung, Taiwan, ROC

ARTICLE INFO

Article history:
Received 12 October 2009
Revised 10 December 2009
Accepted 11 December 2009
Available online 21 December 2009

Keywords:
Helioxanthin derivatives
Hepatitis B virus
Anti-HBV

ABSTRACT

We have previously shown that helioxanthin can suppress human hepatitis B virus gene expression. A series of helioxanthin analogues were synthesized and evaluated for their anti-hepatitis B virus activity. Modifications at the lactone rings and methylenedioxy unit of helioxanthin can modulate the antiviral activity. Among them, compound **32** is the most effective anti-HBV agent. Compound **32** can suppress the secretion of viral surface antigen and e antigen in HepA2 cells with EC_{50} values of 0.06 and 0.14 μM, respectively. Compound **32** not only inhibited HBV DNA with wild-type and lamivudine-resistant strain but also suppressed HBV mRNA, core protein and viral promoters. In this study, a full account of the preparation, structure–activity relationships of helioxanthin analogues, and the possible mechanism of anti-HBV activity of this class of compounds are presented. This type of compounds possesses unique mode of action differing from existing therapeutic drugs. They are potentially new anti-HBV agents.

1. Introduction

Infection of hepatitis B virus (HBV) frequently results in acute and chronic hepatitis which could lead to liver cirrhosis and hepatocellular carcinoma (HCC). Such infection remains a public health problem worldwide. More than 400 million people worldwide are chronically infected with the hepatitis B virus.[1] Though immunization against HBV has been shown as an effective way to prevent chronic HBV infection, yet effective drugs to eradicate HBV in chronic carriers are still urgently needed. The HBV genome is a 3.2 kb partially double-stranded circular DNA with four open reading frames that encode the viral core antigen (HBcAg), the viral DNA polymerase, the viral surface antigen (HBsAg), and the X protein.[2] The HBV genome is transcribed to produce the 3.5-, 2.4-, 2.1-, and 0.7-kb viral RNAs. Synthesis of HBV RNA is under the control of the core, S1, S2 and X promoters, and enhancers, I and II.[3] During the HBV replication, the 3.5 kb mRNA not only serves as the template for reverse transcription but also encodes the viral core protein and the HBV DNA polymerase. HBV-specific protein, RNA, and DNA are all involved in the process of viral replication. The complexity of HBV life cycle provides opportunities as well as challenges in developing effective therapeutic agents for its infection.

Several nucleoside analogues were recently introduced to treat chronic HBV infection. Notable examples include lamivudine [3TC, (−)β-L-2′,3′-dideoxy-3′-thiacytidine],[4] adefovir [PMEA, 9-(2-phosphonylmethoxyethyl) adenine],[5,6] entecavir (BMS-200475, carbocyclic 2′-deoxyguanosine),[7] telbivudine (L-thymidine),[8] and Clevudine [L-FMAU, 1-[(2*S*,3*R*,4*S*,5*S*)-3-fluoro-4-hydroxy-5-(hydroxymethyl)oxolan-2-yl]-5-methylpyrimidine-2,4-dione].[9] Since these drugs mainly targeted the viral polymerase,[10] resistance and cross-resistance against lamivudine (3TC) and adefovir have emerged after only one to two years of treatment.[11,12] Unfortunately, prolonged antiviral therapy is required to eradicate HBV from the chronically infected patients.[13] The point mutations that lead to the emergence of resistance were also identified recently.[14] Since each of the viral replication elements could be targeted to stall HBV production, increasing attention is being focused on finding anti-HBV agents unaffected by resistance problem. Various non-nucleoside analogues, such as heteroarylpyrimidine Bay 41-4109[15] and oxadiazole derivatives,[16] have been reported to inhibit hepatitis B virus replication by depleting the nucleocapsids or reducing the intracellular virion particles. This approach has opened a new avenue in anti-HBV research today. Inspired by these successes, we also attempt to develop non-nucleoside agent

Abbreviations: HE-145, helioxanthin; HBV, hepatitis B virus; HBsAg, HBV surface antigen; HBeAg, HBV e antigen; HBcAg, HBV core protein; 3TC, lamivudine (−)β-L-2′,3′-dideoxy-3′-thiacytidine; S1P, HBV surface promoter I; S2P, HBV surface promoter II; CP, HBV core promoter; XP, HBV X promoter; E/XP, HBV enhancer I; EIA, enzyme immunoassay; ELISA, enzyme-linked immunosorbent assay.

* Corresponding authors. Tel.: +886 2 2826 7117; fax: +886 2 2826 4843 (S.F. Yeh).
E-mail addresses: chl@chem.sinica.edu.tw (C.H. Lin), fyeh@ym.edu.tw (S.F. Yeh).
† These authors contributed equally to this work.

0968-0896/$ - see front matter © 2009 Elsevier Ltd. All rights reserved.
doi:10.1016/j.bmc.2009.12.038

with novel modes of action to overcome the drug resistance problem.

For many years, natural products have been the most abundant and consistently sources in drug discovery. Previously, we reported that a naturally occurring arylnaphthalene lignan, helioxanthin (isolated from *Taiwanina cryptomerioides* Hayata), can effectively inhibit HBV gene expression and replication in human hepatoma cells.[17,18] In searching for more potent anti-HBV drugs, we synthesized numerous helioxanthin analogues with particular emphasis on the modification of the naphthalene rim, lactone, and phenyl ring of parent structure. Herein, we report a full description of the synthesis of helioxanthin analogues and the biological evaluation of their anti-HBV activities. We also demonstrated the antiviral activity of an active analogue (**32**) that rivals the parent compound in its ability to inhibit the levels of HBV DNA, mRNA, viral proteins, and viral promoters.

2. Results

2.1. Synthesis of helioxanthin and its structural analogues

The synthetic exploration is outlined in Schemes 1–5. Several multi-step procedures have been developed for the total synthesis of helioxanthin. These methodologies include a dimerization approach,[19] inter- and intramolecular Diels–Alder reactions,[20–23] and a Pd-catalyzed benzannulation reaction.[19] Among the known procedures for the preparation of helioxanthin **4,** we found that the protocol reported by Charlton and co-workers[24] provides the greatest flexibility necessary for the large scale synthesis of various analogues. In this strategy, piperonal was first converted to acetal **1** by treating with ethylene glycol and catalytic amount of *p*-TsOH·H_2O in refluxing benzene. The labile acetal was immediately lithiated with *n*BuLi at −78 °C. Another portion of piperonal was added to this resulting lithium reagent to produce hydroxyl acetal **2**. This crude hydroxy acetal was converted into a highly reactive benzo[*c*]furan in refluxing AcOH/Ac_2O and this intermediate was trapped in situ by maleic anhydride via Diels–Alder reaction. The Diels–Alder adduct then underwent spontaneous aromatization under the reaction condition to furnish anhydride **3**. When treated with sodium borohydride, the anhydride **3** was reduced to lactone **4** and regio-isomer **5** (retro-helioxanthin). Bromination of **4** with *N*-bromosuccinimide in DMF at room temperature afforded bromo-helioxanthin **6** or **7** depending on the equivalence of NBS used. Further treatment of **6** and **7** with CuCN in DMF gave cyano-helioxanthin **8** and **9**, respectively. Hydrolysis of **4** in basic methanol produced sodium salt **10**. Attempt to fluorinate **4** with *selectfluo*r led to an unexpected oxidation reaction and produced the *ortho*-quinone **11**, instead of the anticipated fluoro-helioxanthin.

Ester **12** was obtained from the esterification of anhydride **3** with catalytic HCl in ethanol. The anhydride **3** was converted to imide **13** by reacting with ethanolamine. Subsequent acetylation of **13** with acetic anhydride in pyridine gave **14**. Reduction of **3** with $LiAlH_4$ led to the diol **15**. Acetylation of **15** gave a mixture of **16** and **17** that was readily separable by flash chromatography. Alcohol **16** was oxidized with PDC in dichloromethane to produce aldehyde **18**. Bromination of diol **15** with PBr_3 gave **19** that was conveniently oxidized to dicarbaldehyde **20** in hot DMSO in the presence of sodium bicarbonate.

To obtain the naphtholic diester **21,** the dienophile in the key Diels–Alder reaction was switched from maleic anhydride to dimethyl acetylenedicarboxylate (DMAD). Hydrolysis in basic methanol removed the less hindered methyl group and produced **22**. Ether **23** was obtained by Williamson's methylation of **21** with CH_3I. Prolonged alkaline hydrolysis of **23** likewise hydrolyzed the less hindered methyl ester and produced compound **24**.

The anhydrides **25–29** were synthesized in similar manner as **3** following Charlton's protocol (Scheme 5). The required hydroxyacetals (**1a–1e**) were synthesized from the lithiated **1** and various known aldehydes. Using maleic anhydride as the dienophile in Diels–Alder reaction, we obtained anhydrides **25–29**. The lactones **30, 33, 36, 39,** and **40** and their retro-isomers **31, 34,** and **37** were obtained by reduction with $NaBH_4$. Selective cleavage of the benzyl protecting group present in lactones **30, 33,** and **36** was carried out with BBr_3 to furnish **32, 35,** and **38**.

2.2. Evaluation of antiviral activities

Human hepatoma cell line, HepA2, was derived from HepG2 cells by transfecting a tandem repeated full-length HBV DNA. HepA2 cells continually synthesize and secrete HBsAg and HBeAg

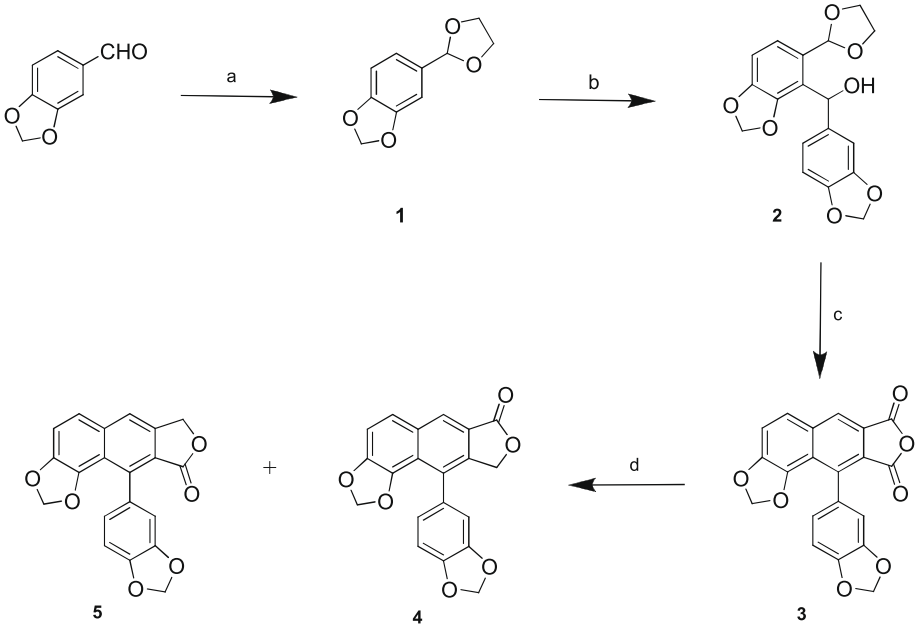

Scheme 1. Reagents and conditions: (a) ethylene glycol, *p*-toluenesulfonic acid, benzene, reflux; (b) *n*-BuLi, piperonal, THF, −78 °C to room temperature; (c) maleic anhydride, AcOH, Ac_2O, CH_2Cl_2, 140 °C, 24 h; (d) $NaBH_4$, THF, room temperature, 2 h.

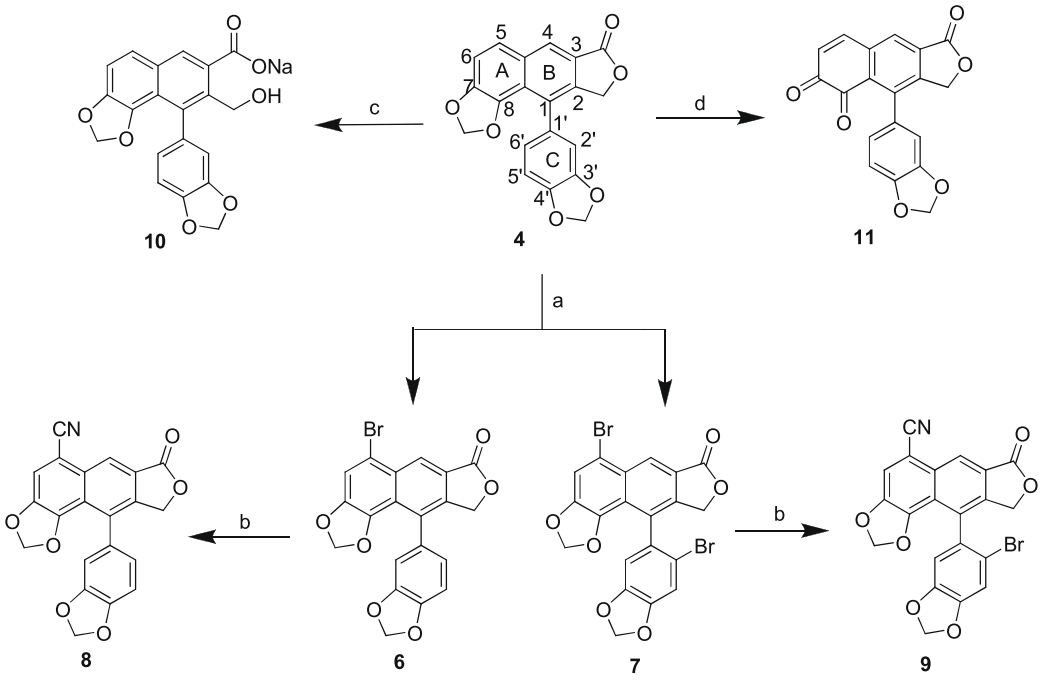

Scheme 2. Reagents and conditions: (a) *N*-bromosuccinimide, DMF, room temperature, 24 h; (b) CuCN, DMF, reflux, 12 h; (c) NaOH, MeOH, reflux, 12 h; (d) selectfluor, CH_3CN, reflux, 24 h.

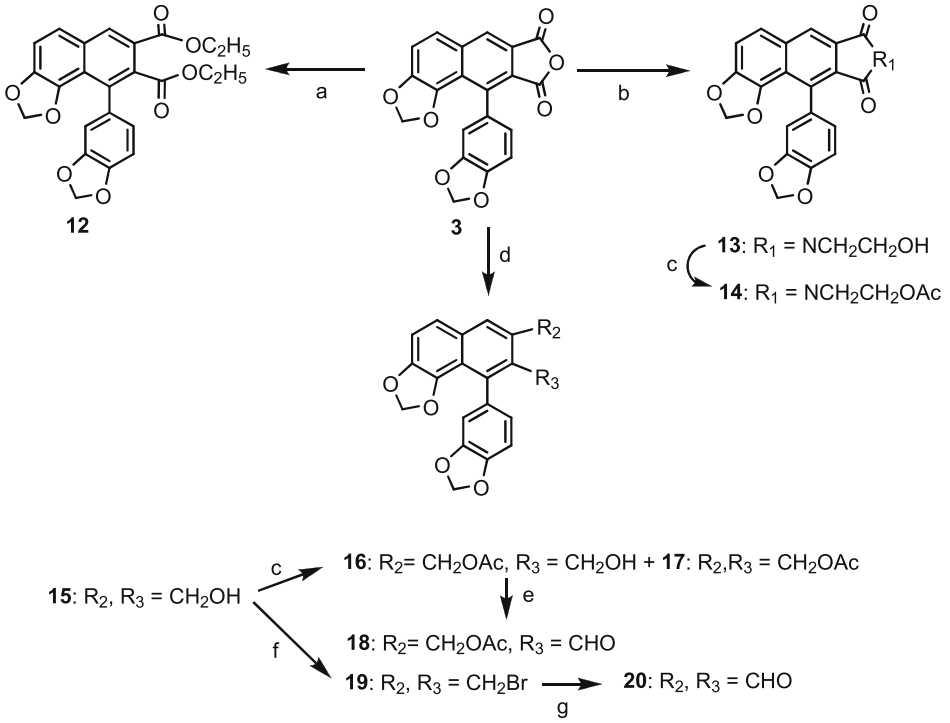

Scheme 3. Reagents and conditions: (a) EtOH, concd HCl, reflux, 12 h; (b) amino ethanol, Et_3N, toluene, reflux, 5 h; (c) Ac_2O, pyridine, room temperature, 12 h; (d) LAH, THF, 0 °C, 1 h; (e) PDC, CH_2Cl_2, room temperature, 1 h; (f) PBr_3, toluene, room temperature to 40 °C, 3 h; (g) $NaHCO_3$, DMSO, 100 °C, 10 min.

into the culture medium. This cell line is an excellent assay system for screening natural or synthetic compounds for anti-HBV activity.[25] We examined helioxanthin and its analogues for their biological activities against human hepatitis B virus. Among all 34 compounds tested, helioxanthin **4** and derivative **32** were found to possess the best activity (EC_{50} = 0.16 μM and 0.14 μM, respectively), whereas retro-isomer **5** (EC_{50} = 2.18 μM) is less active by more than one order of magnitude. Analogues **16** (EC_{50} = 0.42 μM), **10** (EC_{50} = 0.89 μM), **17** (EC_{50} = 1.22 μM), **15** (EC_{50} = 1.41 μM), and **35** (EC_{50} = 1.89 μM) also exhibit antiviral activities against HBV. Moderate to low anti-HBV effects were observed for analogue **20** (EC_{50} = 2.39 μM), **38** (EC_{50} = 3.06 μM), and **39** (EC_{50} = 7.64 μM). All other compounds in this study displayed no detectable anti-HBV activity within the same range of concentrations.

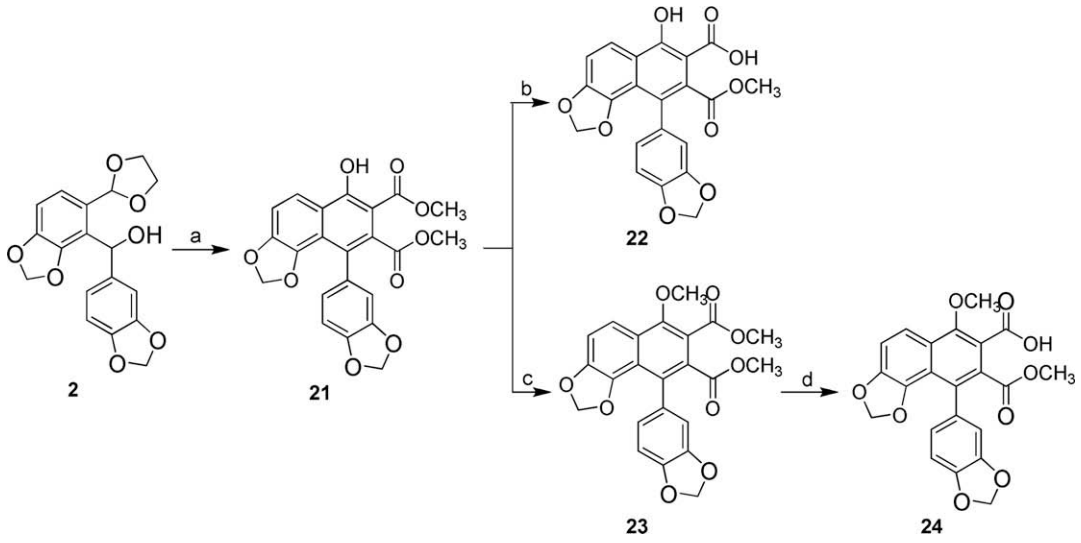

Scheme 4. Reagents and conditions: (a) DMAD, AcOH, Ac_2O, CH_2Cl_2, 140 °C, 24 h; (b) KOH/MeOH, 65 °C, 2 h; (c) CH_3I, K_2CO_3, DMF, room temperature, 3 h; (d) KOH/MeOH, 65 °C, 12 h.

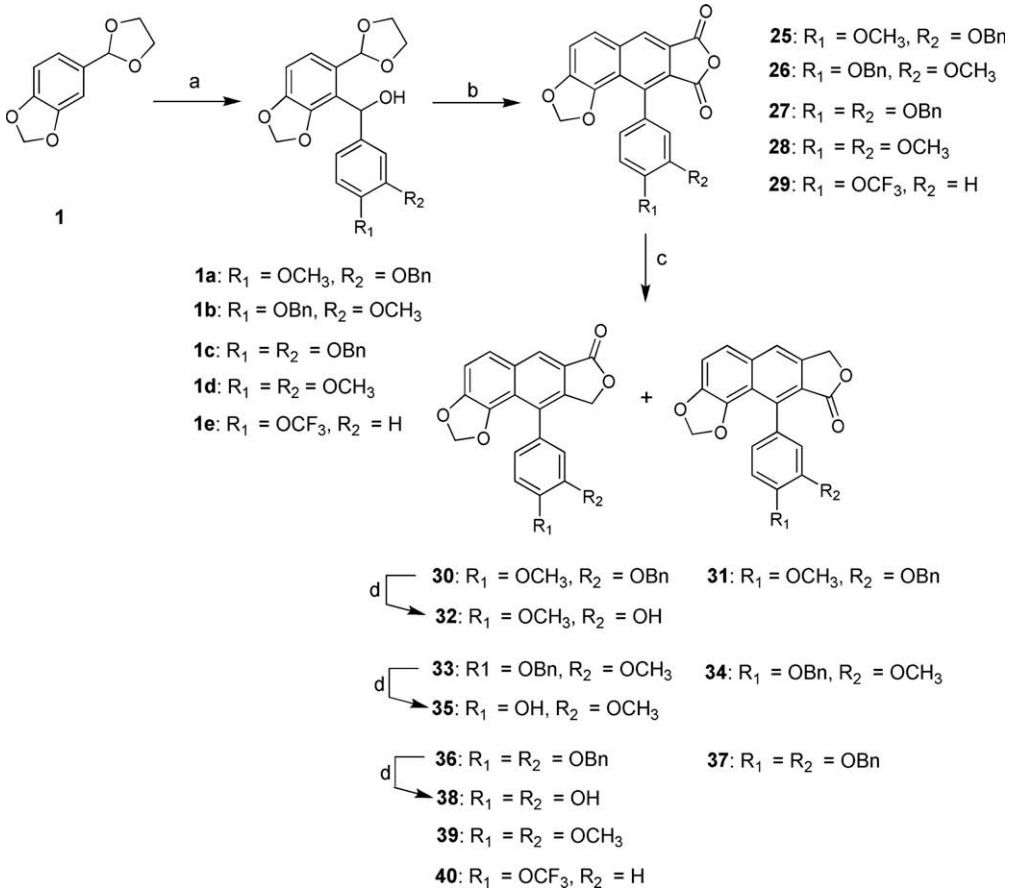

Scheme 5. Reagents and conditions: (a) *n*-BuLi, 3-benzyloxy-4-methoxybenzaldehyde (for **25**) or 4-benzyloxy-3-methoxybenzaldehyde (for **26**) or 3,4-dibenzyloxybenzaldehyde (for **27**) 3,4-dimethoxybenzaldehyde (for **28**) or *p*-trifluoromethoxybenzaldehyde (for **29**), THF, −78 °C to room temperature; (b) maleic anhydride, AcOH, Ac_2O, CH_2Cl_2, 140 °C, 24 h; (c) $NaBH_4$, THF, room temperature, 2 h; (d) BBr_3, CH_2Cl_2, −78 °C, 2 h.

2.3. Compound 32 suppressed HBsAg and HBeAg production in HepA2 cells

Natural product, helioxanthin can suppress both HBsAg and HBeAg production in HepA2 cells.[17] As shown in Table 1, among these synthesized helioxanthin analogues, compound **32** is the most effective in anti-HBsAg production. Further tests were therefore conducted. HepA2 cells were seeded in a 24-well culture plate to which various concentrations of **32** were added. After 48 h of incubation, HBsAg or HBeAg in the media were determined by

Table 1
Biological activity of suppression of HBV surface antigen (HBsAg) of helioxanthin or derivatives in HepA2 cells

Compound	EC_{50}[a]	CC_{50}[b] (μM)	Compound	EC_{50}[a]	CC_{50}[b] (μM)
3	>12.5	11.79 ± 2.10	**21**	>12.5	7.04 ± 1.63
4	0.16 ± 0.03	11.26 ± 1.15	**22**	>12.5	7.01 ± 0.62
5	2.18 ± 1.21	>12.5	**23**	>12.5	8.93 ± 1.19
6	>12.5	6.33 ± 1.82	**24**	>12.5	7.87 ± 0.88
7	>12.5	>12.5	**25**	>12.5	>12.5
8	>12.5	>12.5	**26**	>12.5	11.68 ± 1.37
9	>12.5	>12.5	**27**	>12.5	>12.5
10	0.89 ± 0.12	>12.5	**30**	>12.5	>12.5
11	>12.5	7.49 ± 2.14	**31**	>12.5	>12.5
12	>12.5	>12.5	**32**	0.14 ± 0.02	10.05 ± 1.06
13	>12.5	>12.5	**33**	>12.5	>12.5
14	>12.5	>12.5	**35**	1.89 ± 0.21	>12.5
15	1.41 ± 0.31	>12.5	**36**	>12.5	>12.5
16	0.42 ± 0.21	>12.5	**37**	>12.5	>12.5
17	1.22 ± 0.87	6.91 ± 0.22	**38**	3.06 ± 0.75	7.01 ± 1.19
18	>12.5	4.69 ± 1.70	**39**	7.64 ± 2.04	5.86 ± 1.17
20	2.39 ± 0.53	5.31 ± 0.21	**40**	>12.5	>12.5

Note: Cultured HepA2 cells were seeded on 96-well culture plates and treated with various concentration of compounds in DMEM for 2 days. Cultured cells were collected and the number of cells was examined using MTT assay.
[a] Concentration of suppression of HBsAg at 50% of untreated cells.
[b] Concentration of cell growth at 50% of untreated cells.

ELISA assay. Compound **32** potently suppressed both the endogenously expressed HBsAg and HBeAg production with an EC_{50} about 0.06 μM and 0.14 μM, respectively (Fig. 1). The efficacy of **32** is similar to helioxanthin **4** (Table 1) which was used as a positive control throughout this study. It is worth pointing out that the suppressive activity of **32** on HBsAg and HBeAg production in HepA2 cells is highly specific and is not due to the cytotoxic effect of this compound. The treated cells were viable and continued to proliferate during the 48 h incubation period.

2.4. Compound 32 suppressed viral replication of both wt HBV and lamivudine-resistant HBV

We then tested the effect of **32** on HBV DNA in 1.3ES2 cells (stably transfected with a 1.3-fold wt HBV ayw strain genome[26] in HepG2 cells) and M33 (HepG2 cell line [HBV] containing the lamivudine-resistant HBV with L515M/M539V double mutation in the DNA polymerase region). 1.3ES2 and M33 cells were both treated with various concentrations of **32, 14,** or **4**. After 6 days of treatment, the amount of released viral-associated HBV DNA secreted into the medium was determined using quantitative real-time PCR (Fig. 2). Compound **32** reduced HBV DNA in a dose-dependent manner both in 1.3ES2 and M33 cells. In contrast, lamivudine only showed inhibitory effect in 1.3ES2 but not in M33 cells. The suppression of HBV DNA by the lactone **32** is again structure-specific since the imide analog **14** showed no detectable suppression activity in either 1.3ES2 or M33 cells.

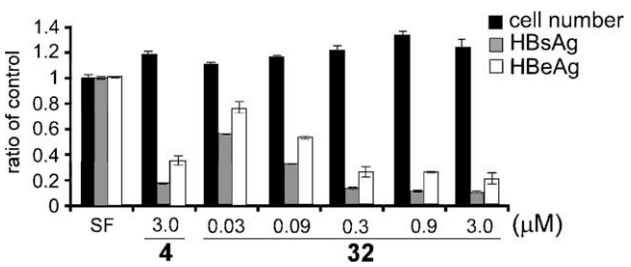

Figure 1. Effects of compound **32** on HBsAg and HBeAg production in HepA2 cells. HepA2 cells were seeded on 24-well plates at a density of 8×10^4 cells/cm^2 in DMEM with 10% fetal calf serum and allowed to attach overnight. The cells were then washed twice with phosphate-buffered saline (pH 7.0) and treated with various concentrations of compound **32** or **4** (3.0 μM in serum-free DMEM for 48 h. The amounts of HBsAg and HBeAg in the culture medium were determined by enzyme immunoassay. Viable cells in each well were determined by the WST-1 assay. Data are expressed as mean ± SD (n = 3).

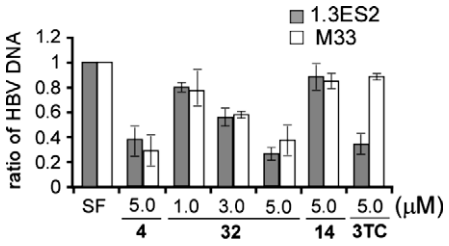

Figure 2. Effects of compound **32** or 3TC treatment on the HBV DNA level in media of 1.3ES2 and M33 cells. Quantitative real-time PCR was used to detect HBV titer in the media of wild (1.3ES2) cells and 3TC-resistant mutant (M33) cells. Cultured cells were seeded on 100 mm culture dishes and treated with various concentrations of compound **32** (1.0, 3.0 and 5.0 μM and 5.0 μM compound **4** or **14** or **3TC** in serum-free (SF) DMEM for 72 h. Media were collected for real-time PCR analysis using primer pair designed against HBV DNA. Data were expressed as mean ± SD (n = 3).

2.5. Compound 32 suppressed all HBV transcripts in 1.3ES2 cells

To determine whether the suppression of viral replication by **32** is mediated through interference with the expression of viral transcripts, total cellular RNA was extracted and examined by Northern blot analysis. 1.3ES2 cells were grown in DMEM with 10% fetal calf serum till confluence. The medium was then changed to serum-free DMEM with various concentrations of **32**, **4,** and **14** for 2 days. As shown in Figure 3, **32** significantly decreased 3.5-kb (HBeAg mRNA and pregenomic RNA) and 2.4/2.1-kb (large HBsAg mRNA and middle/major HBsAg mRNA) HBV transcripts in a dose-dependent manner in 1.3ES2 cells. In contrast, **14** had no such effect on HBV RNA levels.

2.6. Compound 32 reduced HBV core protein levels in 1.3ES2 cells

Since 3.5 kb HBV transcript was decreased after drug treatment, it was anticipated that this class of compounds would also affect viral protein expression. To test this prediction, we treated 1.3ES2 cells with **32**, **14,** and **4** for 2 days and performed Western

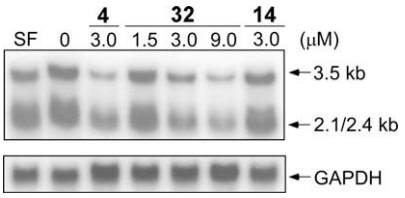

Figure 3. Effects of compound **32** on steady-state mRNA level of HBV RNAs in 1.3ES2 cells. 1.3ES2 cells were seeded on 100 mm culture dishes and treated with various concentration of compound **32** (0, 1.5, 3.0 and 9.0 μM) and 3.0 μM compound **4** or **14** in serum-free DMEM medium for 48 h. Total RNA was extracted from serum free (SF) and compound **32**-treated cells and analyzed by Northern hybridization with HBV DNA probe as described in Section 5. The mRNA of the glyceraldehydes-3-phosphate dehydrogenase (GAPDH) gene was used as an internal marker. Data are representative of three independent experiments.

blot analysis using anti-HBV core protein antibody to examine if the drugs could suppress core protein expression in the cells. As shown in Figure 4, the expression of core protein decreased in a dose-dependent manner upon treatment by compound **32**. On the other hand, **14** exhibited no effect on HBV core protein expression.

2.7. Compound 32 selectively suppresses viral promoter activity for HBV surface antigen, core antigen and enhancer I in HepA2 cells

The observation that **32** effectively reduced the level of viral transcripts raised the possibility that **32** might also affect the viral promoter activity. We examined the activities of four viral promoters including large viral surface antigen (S1P), major viral surface promoter (S2P), viral core protein (CP) and viral X protein (XP). Furthermore, enhancer I (E/XP) was also subjected to the same test. In these experiments, luciferase was used as the reporter assay. As shown in Figure 5, we found that compound **32** and **4** selectively suppressed S1P, S2P, CP, and E/XP activities but has no effect on XP activity in HepA2 cells. None of the promoters or enhancer I activities was suppressed by **14** (Fig. 5).

3. Discussion

3.1. SAR evaluation

Some important structure–activity relationship principles can be deduced from a meticulous analysis of the data listed in Table 1. To simplify the discussion, we first categorized all the synthetic analogues into six classes. In the first type of derivatives (denoted type A), alterations are made on the rim of naphthalene ring. Brominated and cyanated derivatives **6**, **8** both belong to this class. When the lactone moiety of helioxanthin is modified, these analogues are classified as type B. Anhydride **3**, retro-helioxanthin **5**, diester **12**, and diol derivatives **15–20** are examples of this group. Type C compounds are those with structural modifications occur on the phenyl substitution. Compounds **30**, **32**, **33**, **35**, **36**, **38**, **39** and **40** in Scheme 5 are all members of this family. The next three classes of compounds (D, E, and F type, respectively) are consisted of synthetic derivatives with two types of structural modification occur in the same molecule. For example, all compounds in Scheme 4 are modified both on the naphthyl (type A) and lactone ring (type B), and these compounds are classified as type D. Several compounds in Scheme 5 contain alterations both at lactone ring and phenyl substitution and are likewise assigned to type E. Finally, compounds **7** and **9** are modified both on naphthyl and phenyl ring. These two compounds are classified as type F. The complete classification of structural analogues is shown in Table 2.

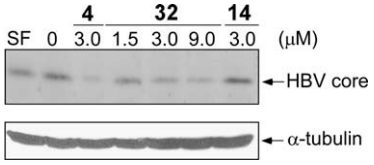

Figure 4. Effects of compound **32** on HBV core protein levels in 1.3ES2 cells. 1.3ES2 cells were seeded on 100 mm culture dishes and treated with various concentration of compound **32** (0, 1.5, 3.0 and 9.0 μM) and 3.0 μM compound **4** or **14** in serum-free (SF) DMEM medium. After 48 h, cell lysates were prepared. Total protein lysates were resolved on SDS–polyacrylamide gel electrophoresis gels and visualized by immunoblotting using a mouse anti-HBV core antibody. The amount of α-tubulin present was also probed as internal controls. Data are representative of three independent experiments.

By correlating the EC_{50} values in Table 1 and the structural categories in Table 2, we found that all compounds belonging to type A, D and F are inactive. The total absence of any antiviral activity in such a wide array of structurally diverse compounds is somewhat surprising at first. However, it is immediately clear that all three types of compounds contain some modification(s) on the naphthyl ring. When this region is modified, even slightly, the antiviral activity vanishes altogether. Whether the incorporated substitution is a hydrogen bonding donor (OH), hydrogen bonding acceptor (CN), or neutral (Br) group makes no difference. It can be reasonably deduced from these observations that the naphthalene rim in helioxanthin is the most tightly bounded area to its target in vivo. Furthermore, to complement the property of this aromatic binding motif, the binding pocket is likely a hydrophobic pocket mostly consisted of aromatic residues. This postulation can be tested with affinity labeling or crystallography in the future.

The other three classes of compounds all contain structural modifications at either the lactone or the phenyl ring. In these 23 synthetic analogues, 10 compounds exhibit antiviral activities. Curiously, all the active compounds belong to B or C type. None of the 5 compounds in type E exhibits any antiviral activity. The most intuitive rationale for this observation is that the in vivo binding sites of both lactone and phenyl rings are relatively flexible. Therefore, minor structural alterations at either site can be made without disrupting the antiviral activity. This loose binding mode is in sharp contrast to the tight binding of naphthyl rim depicted previous. On the other hand, when both the lactone and the phenyl ring are modified (type E), no antiviral activity was detected. From this observation, we can reasonably deduce that the loose binding for these two moieties are somewhat cooperative. Apparently, the overall binding pocket can tolerate certain single site alteration as in type B and C, but the E type 'double mutation' analogues can no longer efficiently bind to their target. Seven of these compounds (**3**, **4**, **6**, **10**, **13**, **21**, and **23**) have been tested against HBV before by Cheng's group.[23] Despite of some numerical difference, the trend observed in the published results is qualitatively consistent with our present data.

A more detailed structure–activity relationship of compounds in type B and C emerged upon closer inspection. We first noticed none of the anhydrides (**3**, **25**–**27**) and imides (**13**, **14**) derivatives exhibits any antiviral activity. An obvious rationale for these results is that these compounds with extra carbonyl groups can not be fitted into the binding pocket and therefore become inactive. Especially, the anhydrides and imides both possess the cyclic dicarbonyl structural motif and the extra carbonyl groups in these compounds always points at a fixed direction due to the rigidity of the five member rings. This explanation sufficiently accounts for why none of the anhydrides and imides derivatives exhibit any activity. However, this overly-simplified explanation did not take into account the moderate activities exhibited by the aldehyde derivative **20**. This peculiarity will be discussed next.

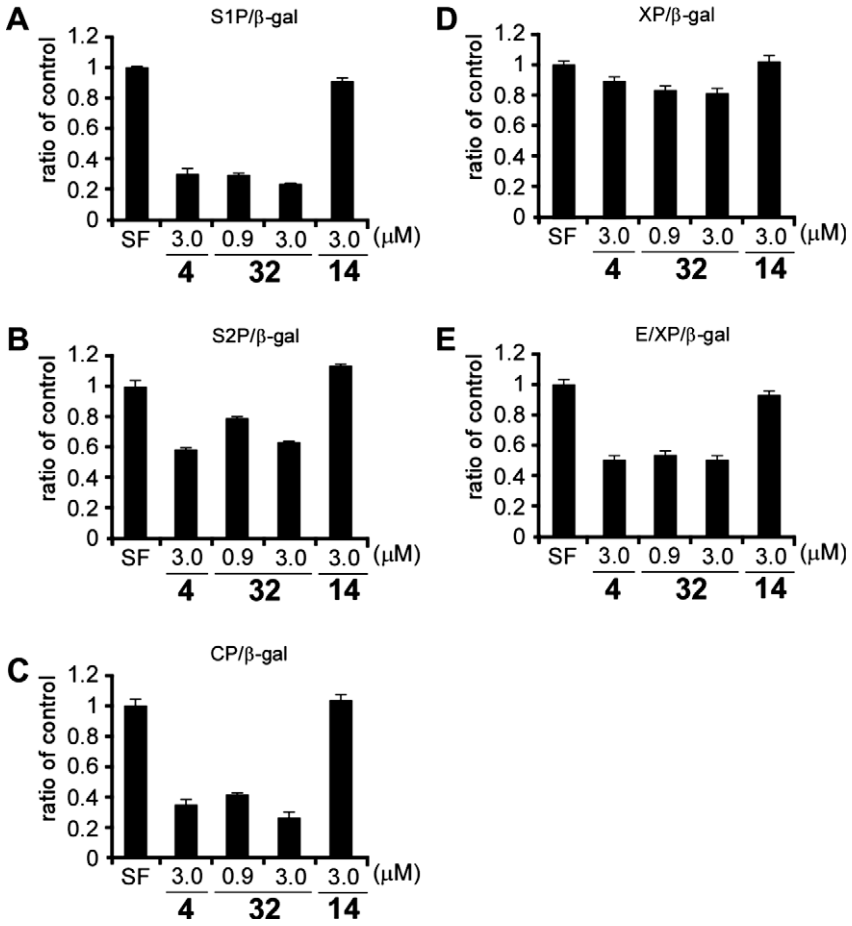

Figure 5. Compound **32** suppresses the promoter activity of HBV in HepA2 cells. Different HBV promoter region were cloned into promoterless mammalian expression vector. HepA2 cells were transfected with S1P (A), S2P (B), CP (C), XP (D) and E/XP (E) of HBV promoter region with luciferase reported gene, respectively. After transfection, HepA2 cells were treated with serum free (SF), compound **32** (0.9 and 3.0 μM) and 3.0 μM compound **4** or **14** in serum-free DMEM for 48 h. The transfection efficiency was corrected by cotransfecting β-gal expression vector and assayed β-gal activity simultaneously. Data were expressed as mean ± SD (n = 3). Data are representative of three independent experiments.

Table 2
Classifications of helioxanthin structural analogues

Classifications	Compounds
Type A derivatives	**6, 8,** and **11**
Type B derivatives	**3, 5, 10, 12, 13, 14, 15, 16, 17, 18,** and **20**
Type C derivatives	**30, 32, 33, 35, 36, 38, 39,** and **40**
Type D derivatives	**21, 22, 23,** and **24**
Type E derivatives	**25, 26, 27, 31,** and **37**
Type F derivatives	**7** and **9**

For other type B derivatives, the lactone rings are all changed to acyclic structures. In these seven compounds (**10, 12, 15, 16, 17, 18,** and **20**), two (**12** and **18**) are inactive. By varying the sizes and polarities at the acyclic terminals and testing the antiviral activities in these compounds, we wished to map the environment in their binding site. However, it is difficult to develop a unified model to explain our observations solely based on the size and polarity of the functional groups. However, we found that data become more intelligible if we assume deacetylation can take place in vivo. For example, if the acetyl groups are readily hydrolyzed in vivo, both **16** and **17** can be simply viewed as masked forms of the active **15**. The slight discrepancy in their activities can be due to the difference in their bio-viability (**15** is relatively insoluble). On the other hand, hydrolysis of the inactive **18** leads only to lactol, an unlikely candidate for antiviral activity. Finally, the two ester groups in **12** are clearly much bulkier than the original lactone and therefore unable to fit into the binding site.

Unlike in type B analogues, the SAR relationship in type C analogues can be explained with structural factors. In these compounds, all the derivatives with the benzyl protecting group still attached (**30**, **33**, and **36**) are inactive. On the contrary, compounds with substitution sizes close to the [1,3] dioxole in helioxanthin (**32** and **35**) are both active. Catechol type derivative **38** and dimethoxy **39** only possess very weak activity. These results indicate that the binding cleft for the phenyl moiety must be quite sensitive to the size of the substrate.

This simple space-fitting model is adequate to account for the general trend of SAR relationship in C type compounds but fails to explain the observed discrepancy in activity between compounds **32** and **35**. As shown in Table 1, compound **32** is 10 times more active than **35** despite them are virtually identical in molecular sizes. The negative result observed in **40** might provide a clue to this puzzle. The lack of activity in this fluorinated derivative strongly suggests that the binding site is not only selective to the sizes, but also sensitive to the surface potentials of the substrates. Since the only notable difference between **32** and **35** is the position of the electropositive H atom, this surface potential sensitive binding model gives a plausible account why **32** is more active than **35**.

The CC_{50} values in Table 1 refer to the cytotoxicity of these synthetic analogues. Although such toxicity data cannot be linked to structural features as we demonstrated for the antiviral activities,

we believe it is still worthwhile to map out a few common structural motifs that might lead to cytotoxicity. Expectedly, compounds with higher antiviral activities (helioxanthin, **17**, and **32**) also exhibit cytotoxic effect. Otherwise, compounds with measurable toxicity always carry functional groups that are considered good electrophiles such as anhydrides in compounds **3** and **21**–**26**, aldehyde in **18** and **20,** and the *ortho*-quinone in **11** (or the *ortho*-quinone precursor in **38**). These reactive groups can all react with various biological nucleophiles and cause adverse effect in vivo. Therefore, it is sensible to avoid these functional groups when optimizing these potential drugs in the future.

In order to clarify whether the molecular mechanism of our most active compound is similar to that of helioxanthin, further studies were performed with **32**. With these investigations, we found **32** can simultaneously decrease the HBV RNA level and core antigen protein expression. Furthermore, inhibition of HBV replication in cell culture was also observed. In short, the treatment of **32** not only reduces the expression of viral transcripts but there was significant decline in the amount of virus production by the cells. Such comprehensive suppression at all levels of viral life cycle is only observed in parent helioxanthin and two other analogues (lactam and piperazine dione derivatives).[18,27] These results demonstrate the likeliness that **32** interferes with viral replication at a very upstream event like helioxanthin. Based on the wide scope of its activity, we propose that **32** suppresses the production of the 3.5-kb pregenomic RNA. Since this key RNA transcript not only encodes the core and polymerase proteins but also serves as a template for reverse transcription, the observed inhibition of RNA transcription and the reduction of core protein level are reasonably attributed as consequence of the suppression 3.5-kb RNA transcription. Moreover, we also observed the interference of viral core promoter activity by **32** (Fig. 4). Therefore, the reduction of 3.5 kb HBV pregenomic RNA production is most like the result of blocked CP activity. These results foretold our observations that **32** can decrease HBV viral particle production by 1.3ES2 cells (Fig. 2). Based on these observations, we propose the anti-HBV activity of **32** is most likely the result of interference with the transcriptional machinery as been observed before in **4** and its lactam analogue.[17,18,27] The mechanistic similarity with helioxanthin **4** firmly establishes this class of natural product as effective anti-HBV drugs or lead compounds. In addition, the core protein level was also decreased after the treatment of **32** (Fig. 4). However, it remains unclear whether this reduction in core protein is the cause or the consequence of the reduction in capsid formation by **32**.

In addition to the antiviral activity against simple wild-type HBV, we also evaluated the activity of **32** against lamivudine-resistant HBV that contained L515M and M539V double mutations in the polymerase protein. To our delight, we found the lamivudine-resistant M33 mutant strain was still sensitive to treatment by **32**. This result highlighted the potential of this class of natural product in long-term anti-HBV therapy or combination therapy.

In conclusion, through our synthetic effort and biological testing, a model of structure–activity relationship in this class of compounds is proposed for the first time. Although the analogues reported here are only comparable to the parent compound **4** at best, the established structure–activity relationship can be a valuable guide in further design nonetheless. For example, C type derivatization can be a versatile handle for improving drug stability and bio-viability. Like the lead compound helioxanthin, compound **32** not only reduces HBV DNA but also decreases HBV RNA, HBV core protein expression. **32** also inhibits the activity of HBV viral promoters and enhancer to affect the viral replication in human hepatoma cells. The mode of action for **32** should be similar to that of parent helioxanthin and its lactam analogous[17,27] while differ considerably from the existing therapeutic drugs like 3TC. The uniqueness of these new anti-HBV agents make **32** another worthy candidate for further antiviral combination therapy. For example, a combined dosage of **32** and 3TC might eradicate HBV infection in a relatively short time before the virus can develop resistance to the latter. Alone this direction, we are currently testing these compounds as novel anti-HBV agents in HBV transgenic mice and the results will be reported in due course.

4. Experimental section

4.1. General methods for synthesis

All reactions are performed under 1 atmosphere of dried nitrogen and well mixed with magnetic stirring devices. Reagent grade chemicals and solvents were used in all reactions. Reaction vessels were dried in oven before use. Diethyl ether and tetrahydrofuran were distilled over metallic sodium with benzophenone radical anion as the indicator. Dichloromethane were distilled from CaH_2. Flash column chromatography was performed with Silica Gel 60 (0.040–0.063 mm) as the stationary phase. All ratios of reported mixed eluents are based on volume.

Anhydride **3**, helioxanthin **4,** and its retro-isomer **5** were synthesized according to the literature procedure.[23]

4.1.1. 10-Benzo[1,3]dioxol-5-yl-5-bromo-9*H*-furo[3′,4′:6,7]naphtho-[1,2-*d*][1,3]dioxol-7-one (6)

To a solution of **4** (100 mg, 0.29 mmol) in DMF (5 ml) was added *N*-bromosuccinimide (77 mg, 0.43 mmol). The mixture was stirred for 24 h at room temperature. After the completion of the reaction, the reaction mixture was diluted with CH_2Cl_2 and washed with water (3×25 ml). The organic fraction was dried over $MgSO_4$ and concentrated. After column chromatography (hexane/CH_2Cl_2 = 1:1), yellow solid **6** (89 mg, 74%) was isolated. ^{1}H NMR (500 MHz, $CDCl_3$) δ: 8.86 (s, 1H), 7.62 (s, 1H), 6.86 (d, J = 7.6 Hz, 1H), 6.73–6.75 (m, 2H), 6.04 (dd, J = 1.3, 11.2 Hz, 2H), 5.93 (dd, J = 1.4, 10.0 Hz, 2H), 5.18 (AB, J = 15.2 Hz, 2H). ^{13}C NMR (100 MHz, $CDCl_3$) δ: 170.7, 147.6, 146.6, 141.8, 140.5, 140.5, 129.9, 129.9, 128.9, 127.2, 122.4, 122.3, 122.3, 117.4, 116.2, 109.5, 108.1, 102.0, 101.3, 69.3. IR (CH_2Cl_2, cast): 1762, 1624, 1446, 1308, 1234, 1134, 1074, 1041, 758. FAB-LRMS *m/z* (rel intensity): 426 (M^+, 4), 419 (11), 417 (1), 391 (68), 389 (5), 341 (2), 340 (1), 279 (12), 267 (8), 209 (9), 194 (3), 167 (18). FAB-HRMS Calcd for $C_{20}H_{11}O_6Br$ *m/z*: 425.9737 $[M]^+$, found 425.9729.

4.1.2. 5-Bromo-10-(6-bromo-benzo[1,3]dioxol-5-yl)-9*H* -furo-[3′,4′:6,7]naphtha[1,2-*d*][1,3]dioxol-7-one (7)

To a solution of **4** (100 mg, 0.29 mmol) in DMF (5 ml) was added N-bromosuccinimide (127 mg, 0.71 mmol) and the reaction was treated as described for **6**. After column chromatography (hexane/CH_2Cl_2 = 1:1), **7** (100 mg, 70%) was isolated as a yellow powder. ^{1}H NMR (400 MHz, $CDCl_3$) δ: 8.89 (s, 1H), 7.62 (s, 1H), 7.10 (s, 1H), 6.71 (s, 1H), 6.07 (dd, J = 1.2, 6.8 Hz, 2H), 5.94 (dd, J = 1.3, 9.6 Hz, 2H), 5.12 (s, 2H). ^{13}C NMR (125 MHz, $CDCl_3$) δ: 170.6, 148.7, 147.2, 146.6, 141.7, 140.6, 129.9, 128.7, 128.7, 127.8, 122.4, 122.2, 117.4, 116.3, 114.2, 112.5, 109.8, 102.4, 102.2, 69.1. IR (KBr): 1762, 1627, 1476, 1421, 1310, 1232, 1133, 1070, 1021. FAB-LRMS *m/z* (rel intensity): 503 (M^+, 6), 427 (1), 391 (4), 341 (1), 173 (3). FAB-HRMS Calcd for $C_{20}H_{10}O_6Br_2$ *m/z*: 503.8844 $[M]^+$, found 503.8859.

4.1.3. 10-Benzo[1,3]dioxol-5-yl-7-oxo-7,9-dihydro-furo-[3′,4′:6,7]naphtho[1,2-*d*][1,3]dioxole-5-carbonitrile (8)

CuCN (100 mg, 1.12 mmol) was added to a solution of **6** (50 mg, 0.12 mmol) in DMF (5 ml) and the resulting mixture was refluxed for 12 h. The reaction mixture was quenched with brine (25 ml) and extracted with ether (25 ml). The extract was dried over

$MgSO_4$ and concentrated. After column chromatography (hexane/CH_2Cl_2 = 1:3), pure **8** (33 mg 76%) was isolated as a yellow solid. ^1H NMR (400 MHz, $CDCl_3$) δ: 8.80 (s, 1H), 7.65 (s, 1H), 6.88 (dd, J = 1.1, 7.2 Hz, 1H), 6.75 (s, 1H), 6.73 (d, J = 1.6 Hz, 1H), 6.06 (dd, J = 1.3, 4.0 Hz, 2H), 6.03 (dd, J = 1.3, 3.8 Hz, 2H), 5.19 (AB, J = 15.4 Hz, 2H). ^{13}C NMR (100 MHz, $CDCl_3$) δ: 169.8, 147.9, 147.6, 146.7, 145.8, 141.2, 131.3, 130.9, 129.2, 124.4, 124.0, 122.2, 121.1, 117.2, 117.1, 109.3, 108.2, 105.7, 102.9, 101.5, 101.4, 69.3. IR (CH_2Cl_2, cast): 2212, 1765, 1606, 1496, 1446, 1312, 1237, 1081, 1031 cm^{-1}. FAB-LRMS *m/z* (rel intensity): 373 (M^+, 46), 344 (13), 327 (26), 281 (14), 267 (10), 207 (17), 136 (100). FAB-HRMS Calcd for $C_{21}H_{11}O_6N$ *m/z*: 373.0586 $[M]^+$, found 373.0589.

4.1.4. 10-(6-Bromo-benzo[1,3]dioxol-5-yl)-7-oxo-7,9-dihydro-furo[3′,4′:6,7]naphtha[1,2-*d*][1,3]dioxole-5-carbonitrile (9)

CuCN (180 mg, 2 mmol) was added to a solution of **7** (100 mg, 0.2 mmol) in DMF (10 ml) and the reaction was treated as described for **8**. After column chromatography (hexane/CH_2Cl_2 = 1:2), pure **9** (30 mg, 34%) was isolated as a yellow powder. ^1H NMR (400 MHz, $CDCl_3$) δ: 8.86 (s, 1H), 7.67 (s, 1H), 7.11 (s, 1H), 6.71 (s, 1H), 6.03–6.09 (m, 4H), 5.14 (s, 2H). ^{13}C NMR (100 MHz, $CDCl_3$) δ: 169.7, 149.0, 147.5, 146.5, 145.8, 141.3, 131.4, 129.7, 129.3, 125.2, 124.2, 117.4, 117.0, 114.1, 112.7, 109.6, 106.0, 103.2, 102.3, 69.1. IR (CH_2Cl_2, cast): 2219, 1765, 1620, 1475, 1312, 1234, 1078, 1035 cm^{-1}. FAB-LRMS *m/z* (rel intensity): 452 ($[M+H]^+$, 18), 417 (2), 409 (16), 391 (5), 373 (18), 343 (3), 329 (2), 258 (4), 195 (4), 178 (4), 120 (12). FAB-HRMS Calcd for $C_{21}H_{10}O_6NBr$ *m/z*: 451.9770 $[M+H]^+$, found 451.9777.

4.1.5. 9-Benzo[1,3]dioxol-5-yl-8-hydroxymethyl-naphtho[1,2-*d*][1,3]-dioxole-7-carboxylic acid monosodium salt (10)

To a hot methanol solution of **4** (50 mg, 0.14 mmol in 2 mL) was added a methanol solution of NaOH (37 mg, 0.92 mmol in 2 mL). The mixture was refluxed overnight. After the completion of the reaction, the solution was concentrated under reduced pressure to give the 100 mg of **10**. Phosphate buffer of pH 7.0 was added to neutralize the excess NaOH in the product. ^1H NMR (300 MHz, D_2O) δ: 7.72 (s, 1H), 7.00 (d, J = 7.6 Hz, 1H), 6.58 (d, J = 8.1 Hz, 1H), 6.41 (d, J = 7.1 Hz, 1H), 6.21 (s, 1H), 6.15 (d, J = 6.8 Hz, 1H), 5.44–5.50 (m, 2H), 5.09 (s, 2H), 4.05 (s, 2H). ^{13}C NMR (125 MHz, D_2O) δ: 176.9, 146.2, 144.6, 140.5, 134.6, 134.0, 133.9, 132.9, 129.6, 128.6, 123.3, 123.2, 119.2, 110.9, 110.4, 107.2, 100.8, 100.5, 59.5. IR (CH_2Cl_2, cast): 3431, 1756, 1631, 1494, 1439, 1266, 1229, 1070, 1030, 919, 801 cm^{-1}.

4.1.6. 4-Benzo[1,3]dioxol-5-yl-3*H*-naphtho[2,3-*c*]furan-1,5,6-trione (11)

A solution of Selectfluor [1-(chloromethyl)-4-fluoro-1,4-diazoniabicyclo[2.2.2]octane bis (tetrafluoroborate)] (51 mg, 0.14 mmol) in acetonitrile (1.5 ml) was added to a solution of **4** (50 mg, 0.14 mmol) in the same medium (5 ml). The resulting mixture was refluxed for 24 h. The solution was then poured into ether (25 ml), washed with water (25 ml) and saturated $NaHCO_3$ (20 ml). The ether fraction was dried over $MgSO_4$, filtered, and concentrated. Pure **11** (29 mg, 60%) was isolated as a dark solid after column chromatography (hexane/CH_2Cl_2 = 1:3). ^1H NMR (500 MHz, $CDCl_3$) δ: 7.87 (s, 1H), 7.59 (d, J = 10.1 Hz, 1H), 6.88 (d, J = 8.3 Hz, 2H), 6.60–6.61 (m, 2H), 6.56 (d, J = 10.1 Hz, 1H), 6.02 (s, 2H), 5.11 (br d, J = 14.5 Hz, 2H). ^{13}C NMR (125 MHz, $CDCl_3$) δ: 180.1, 179.6, 169.0, 149.7, 148.4, 148.2, 145.2, 141.8, 137.3, 132.8, 130.8, 128.8, 128.5, 126.2, 120.4, 109.1, 107.8, 101.5, 69.8. IR (CH_2Cl_2, cast): 1765, 1670, 1617, 1496, 1450, 1301, 1234, 1035, 925; 804 cm^{-1}. FAB-LRMS *m/z* (rel intensity): 336 (M^+, 38), 189 (7), 165 (12). FAB-HRMS Calcd for $C_{19}H_{12}O_6$ *m/z*: 336.0634 $[M]^+$, found 336.0640.

4.1.7. 9-Benzo[1,3]dioxol-5-yl-naphtho[1,2-*d*][1,3]dioxole-7,8-dicarbaxylic acid diethyl ester (12)

Compound **3** was dissolved in ethanol (10 ml) and concentrated HCl (five drops) was added. The mixture was refluxed overnight. After the reaction was cooled to room temperature, saturated $NaHCO_3$ (40 ml) was added and product was extracted with CH_2Cl_2 (50 ml). The organic fraction was dried over $MgSO_4$ and concentrated. After column chromatography (CH_2Cl_2), pure **12** (100 mg, 83%) was isolated. ^1H NMR (500 MHz, $CDCl_3$) δ: 8.50 (s, 1H), 7.56 (d, J = 8.5 Hz, 1H), 7.25 (d, J = 8.2 Hz, 1H), 6.80 (s, 1H), 6.77 (d, J = 1.8 Hz, 2H), 6.01 (d, J = 1.1 Hz, 1H) 5.96 (d, J = 1.1 Hz, 1H), 5.86 (dd, J = 1.2, 10.5 Hz, 2H), 4.36 (q, J = 7.1 Hz, 2H), 4.08 (q, J = 7.1 Hz, 2H), 1.37 (t, J = 7.1 Hz, 3H), 1.06 (t, J = 7.1 Hz, 3H). ^{13}C NMR (100 MHz, $CDCl_3$) δ: 168.5, 165.6, 147.1, 147.0, 146.4, 142.2, 133.4, 132.4, 132.4, 131.2, 128.8, 124.4, 123.5, 122.5, 120.5, 112.0, 110.9, 107.0, 101.5, 100.9, 61.4, 61.1, 14.2, 13.8. IR (CH_2Cl_2, cast): 1737, 1599, 1489, 1446, 1372, 1326, 1234, 1070, 1039, 929 cm^{-1}. FAB-LRMS *m/z* (rel intensity): 436 (M^+, 100), 435 (20), 377 (18), 376 (5), 317 (21), 287 (17), 275 (7), 259 (6), 189 (10), 109 (38). FAB-HRMS Calcd for $C_{24}H_{20}O_8$ *m/z*: 436.1158 $[M^+]$, found 436.1150.

4.1.8. 10-Benzo[1,3]dioxol-5-yl-8-(2-hydroxy-ethyl)-1,3-dioxa-8-aza-dicyclopenta[*a*,*g*]naphthalene-7,9-dione (13)

Compound **3** (200 mg, 0.55 mmol), amino ethanol (37 mg, 0.6 mmol), and triethylamine (5 mg, 0.05 mmol) were dissolved in toluene (10 ml) and water was removed under reflux condition with a Dean–Stark apparatus. After 5 h, the reaction mixture was cooling to room temperature and concentrated under reduced pressure. The residue was triturated with 0.1 N HCl before saturated $NaHCO_3$ was added. The crude mixture was extracted with dichloromethane. The organic fraction was dried over $MgSO_4$ and concentrated. After column chromatography (CH_2Cl_2/ether = 1:5), pure **13** (140 mg, 64%) was isolated. ^1H NMR (500 MHz, $CDCl_3$) δ: 8.24 (s, 1H), 7.64 (d, J = 8.5 Hz, 1H), 7.32 (d, J = 8.4 Hz, 1H), 6.87 (d, J = 7.7 Hz, 2H), 6.79–6.82 (m, 2H), 6.06 (s, 1H), 6.01 (s, 1H), 5.92 (d, J = 9.0 Hz, 2H), 3.85–3.83 (m, 4H), 2.31 (br s, 1H). ^{13}C NMR (50 MHz, $CDCl_3$) δ: 170.9, 167.4, 166.8, 147.7, 147.6, 146.8, 144.6, 136.3, 131.2, 129.1, 125.4, 125.3, 124.5, 122.8, 121.4, 113.1, 109.9, 107.4, 101.9, 101.1, 61.4, 37.1. IR (CH_2Cl_2, cast): 3482, 1758, 1702, 1624, 1492, 1439, 1290, 1230 cm^{-1}. FAB-LRMS *m/z* (rel intensity): 406 ($[M+H]^+$, 13), 405 (8), 371 (1). FAB-HRMS Calcd for $C_{22}H_{16}O_7N$ *m/z*: 406.0927 $[M+H]^+$, found 406.0923.

4.1.9. Acetic acid 2-(10-Benzo[1,3]dioxol-5-yl-7,9-dioxo-7,9-dihydro-1,3-dioxa-8-aza-dicyclopenta[*a*,*g*]naphthalene-8-yl)-ethyl ester (14)

To a solution of **13** (30 mg, 0.074 mmol) in pyridine (2 ml) was added acetic anhydride (15 mg, 0.15 mmol) and the resulting mixture was stirred at room temperature for 16 h. 10% HCl (10 ml) was then added to the reaction and the mixture was extracted with CH_2Cl_2 (20 ml). The organic extract was dried over $MgSO_4$ and concentrated. After column chromatography (hexane/CH_2Cl_2 = 1:3), compound **14** (20 mg, 61%) was isolated as a yellow solid. ^1H NMR (200 MHz, $CDCl_3$) δ: 8.24 (s, 1H), 7.63 (d, J = 8.5 Hz, 1H), 7.31 (d, J = 8.5 Hz, 1H), 6.77–6.88 (m, 3H), 6.00–6.05 (m, 2H), 5.92 (d, J = 3.1 Hz, 2H), 4.26 (t, J = 5.3 Hz, 2H), 3.88 (t, J = 5.3 Hz, 2H), 1.98 (s, 3H). ^{13}C NMR (100 MHz, $CDCl_3$) δ: 170.8, 167.3, 166.8, 147.7, 147.5, 146.8, 144.6, 136.3, 131.2, 129.0, 125.4, 125.2, 125.1, 124.5, 122.7, 121.4, 113.0, 109.8, 107.4, 101.9, 101.1, 61.3, 37.0, 20.7; IR (CH_2Cl_2, cast) 1707, 1649, 1544, 1501, 1454, 1378, 1288, 1230, 1035 cm^{-1}. FAB-LRMS *m/z* (rel intensity): 448 ($[M+H]^+$, 24), 447 (22), 406 (5), 338 (4), 374 (2), 373 (2), 341 (1), 329 (1), 257 (2), 195 (2), 120 (10). FAB-HRMS Calcd for $C_{24}H_{18}O_8N$ *m/z*: 448.1032 $[M+H]^+$, found 448.1024.

4.1.10. (9-Benzo[1,3]dioxol-5-yl-7–dihydroxmethyl-naphtho[1,2-*d*][1,3]dioxol-8-yl)-methanol (15)

A solution of lithium aluminum hydride (22 mg, 0.58 mmol) in THF (95 ml) was cooled to 0 °C in an ice bath and a THF solution of **3** (100 mg, 0.29 mmol in 5 mL) was added. The mixture was stirred for 1 h at the same temperature. Water and a few drops of concentrated sulfuric acid were then slowly added. The mixture was then extracted with CH_2Cl_2. The organic fraction was dried over $MgSO_4$ and concentrated under reduced pressure to give almost pure **15**. After column chromatography (CH_2Cl_2), **15** (90 mg, 89%) was isolated as a white solid. ^{1}H NMR (400 MHz, $CDCl_3$) δ: 7.76 (s, 1H), 7.40 (d, J = 8.5 Hz, 1H), 7.16 (d, J = 8.5 Hz, 1H), 6.83 (d, J = 7.8 Hz, 1H), 6.76 (d, J = 1.3 Hz, 1H), 6.72 (dd, J = 1.5, 7.8 Hz, 1H), 6.04 (d, J = 1.2 Hz, 1H), 6.00 (d, J = 1.2 Hz, 1H), 5.78 (dd, J = 1.4, 5.4 Hz, 2H), 4.89 (s, 2H), 4.59 (AB, J = 11.9 Hz, 2H), 2.11 (br s, 2H). ^{13}C NMR (100 MHz, $CDCl_3$) δ: 146.9, 146.8, 144.9, 142.2, 135.8, 135.5, 135.1, 133.7, 129.6, 129.5, 123.1, 122.1, 119.7, 111.1, 110.5, 107.4, 100.9, 65.3, 59.9. IR (CH_2Cl_2, cast): 3326, 1485, 1443, 1322, 1269, 1234, 1042, 932 cm^{-1}. FAB-LRMS *m/z* (rel intensity): 352 (M^+, 42), 335 (13), 109 (33); FAB-HRMS Calcd for $C_{20}H_{16}O_6$ *m/z*: 352.0947 $[M]^+$, found 352.0943. Anal. Calcd for $C_{20}H_{16}O_6$: C, 68.18; H, 4.58. Found: C, 67.29; H, 4.72.

4.1.11. Acetic acid 9-benzo[1,3]dioxol-5-yl-8-hydroxmethyl-naphtho[1,2-*d*][1,3]dioxol-7-yl methyester (16)

To a solution of **15** (20 mg, 0.056 mmol) in pyridine (3 ml) was added acetic anhydride (6 mg, 0.056 mmol) and the resulting mixture was stirred at room temperature for 16 h. After the completion of the reaction, 10% HCl (5 ml) was added and the mixture was extracted with ether (10 ml). The ether extract was washed with saturated $NaHCO_3$ (5 ml), dried over $MgSO_4$, and concentrated. After column chromatography (hexane/CH_2Cl_2 = 3:1), **16** (16 mg, 73%) was isolated as a colorless solid. ^{1}H NMR (400 MHz, $CDCl_3$) δ: 7.79 (s, 1H), 7.39 (d, J = 8.6 Hz, 1H), 7.15 (d, J = 8.5 Hz, 1H), 6.81 (d, J = 7.8 Hz, 1H), 6.76 (d, J = 1.4 Hz, 1H), 6.71 (dd, J = 1.6, 7.8 Hz, 1H), 6.02 (d, J = 1.2 Hz, 1H), 5.98 (d, J = 1.2 Hz, 1H), 5.76 (dd, J = 1.4, 5.6 Hz, 2H), 5.39 (s, 2H), 4.51 (AB, J = 11.8 Hz, 2H), 2.10 (s, 3H), 1.91 (br s, 1H). ^{13}C NMR (100 MHz, $CDCl_3$) δ: 170.7, 146.9, 146.9, 145.0, 141.9, 135.7, 135.4, 132.9, 130.2, 129.5, 123.1, 123.1, 122.3, 119.9, 111.2, 110.5, 107.4, 101.0, 65.1, 59.2, 21.7. IR (CH_2Cl_2, cast): 3439, 1737, 1599, 1453, 1375, 1234, 1042, 748 cm^{-1}. FAB-LRMS *m/z* (rel intensity): 394 (M^+, 100), 377 (12), 335 (23), 275 (8), 189 (7), 109 (19). FAB-HRMS Calcd for $C_{22}H_{18}O_7$ *m/z*: 394.1053 $[M]^+$, found 394.1057. Anal. Calcd for $C_{22}H_{18}O_7$: C, 67.00; H, 4.60. Found: C, 66.53; H, 4.72.

4.1.12. Acetic acid 8-acetoxymethyl-9-benzo[1,3]dioxol-5-yl-naphtho[1,2-*d*][1,3]dioxol-7-yl methy ester (17)

To a solution of compound **15** (30 mg, 0.085 mmol) in pyridine (5 ml) was added acetic anhydride (18 mg, 0.17 mmol) and the reaction was treated as described for **16**. After column chromatography (hexane/CH_2Cl_2 = 1:4), pure **17** (20 mg, 70%) was isolated as a colorless solid. ^{1}H NMR (400 MHz, $CDCl_3$) δ: 7.81 (s, 1H), 7.42 (d, J = 8.5 Hz, 1H), 7.18 (d, J = 8.5 Hz, 1H), 6.79 (d, J = 7.8 Hz, 1H), 6.72 (d, J = 1.5 Hz, 1H), 6.67 (dd, J = 1.65, 7.8 Hz, 1H), 6.03 (d, J = 1.4 Hz, 1H), 5.99 (d, J = 1.4 Hz, 1H), 5.78 (dd, J = 1.4, 5.5 Hz, 2H), 5.27 (s, 2H), 4.99 (s, 2H), 2.09 (s, 3H), 2.00 (s, 3H). ^{13}C NMR (100 MHz, $CDCl_3$) δ: 170.7, 170.5, 146.9, 146.8, 145.2, 141.9, 137.4, 132.4, 130.5, 130.2, 130.1, 129.7, 123.1, 122.3, 119.7, 111.5, 110.4, 107.4, 101.1, 100.9, 64.8, 61.3, 21.0, 20.9. IR (CH_2Cl_2, cast): 1720, 1624, 1485, 1443, 1262, 1204, 1148, 1070, 1031, 929, 801 cm^{-1}. FAB-LRMS *m/z* (rel intensity): 436 (M^+, 100), 391 (55), 363 (11), 333 (94), 261 (3), 176 (2). FAB-HRMS Calcd for $C_{24}H_{20}O_8$ *m/z*: 436.1158 $[M]^+$, found 436.1150. Anal. Calcd for $C_{24}H_{20}O_8$: C, 66.05; H, 4.62. Found: C, 66.20; H, 4.86.

4.1.13. Acetic acid 9-benzo[1,3]dioxol-5-yl-8-formyl-naphtho[1,2-*d*][1,3]dioxol-7-yl methyl ester (18)

Compound **16** (10 mg, 0.025 mmol) was dissolved in CH_2Cl_2 (5 ml) and pyridinium dichromate was added (43 mg, 0.11 mmol). The reaction mixture was stirred for 1 h at room temperature. The reaction mixture was then filtered and washed thoroughly with CH_2Cl_2 (10 ml). The organic solution was dried over $MgSO_4$ and concentrated. After column chromatography (hexane/CH_2Cl_2 = 1:3), pure **18** (7 mg, 70%) was isolated. ^{1}H NMR (400 MHz, $CDCl_3$) δ: 9.87 (s, 1H), 7.80 (s, 1H), 7.45 (d, J = 8.5 Hz, 1H), 7.28 (d, J = 8.5 Hz, 1H), 6.82–6.85 (m, 2H), 6.76 (dd, J = 1.6, 7.8 Hz, 1H), 6.07 (d, J = 1.2 Hz, 1H), 6.02 (d, J = 1.2 Hz, 1H), 5.86 (dd, J = 1.2, 10.3 Hz, 2H), 5.56 (s, 2H), 2.15 (s, 3H). ^{13}C NMR (100 MHz, $CDCl_3$) δ: 194.0, 170.7, 147.6, 147.1, 145.6, 143.5, 143.0, 130.9, 130.9, 130.1, 129.6, 128.4, 124.3, 122.4, 118.9, 113.4, 110.9, 107.5, 101.5, 101.3, 64.7, 21.1; IR (CH_2Cl_2, cast) 1730, 1680, 1585, 1446, 1372, 1234, 1039, 925 cm^{-1}. FAB-LRMS *m/z* (rel intensity): 392 (M^+, 47), 391 (19), 333 (55), 332 (11), 289 (12), 255 (43), 239 (24), 185 (42), 173 (100), 105 (69). FAB-HRMS Calcd for $C_{22}H_{16}O_7$ *m/z*: 392.0896 $[M]^+$, found 392.0895. Anal. Calcd for $C_{24}H_{20}O_8$: C, 66.05; H, 4.62. Found: C, 66.20; H, 4.86.

4.1.14. 9-Benzo[1,3]dioxol-5-yl-7,8-bis-bromomethyl-naphtho[1,2-*d*][1,3]dioxole (19)

To a stirred solution of **15** (200 mg, 0.57 mmol) in dry toluene (10 ml) was slowly added a solution of phosphorous tribromide (218 mg, 0.80 mmol) in dry toluene (2 ml). After the addition was completed (30 min), the mixture was stirred for 1 h at room temperature and then an additional 2 h at 40 °C. The mixture was then poured into ice and extracted with ether (50 ml). The combined organic extracts was washed with brine (50 ml) and dried over $MgSO_4$. Crude **19** was obtained (200 mg, 74%) after the solvent was removed in vacuo. This crude product was used in the next step directly without further purification.

4.1.15. 9-Benzo[1,3]dioxol-5-yl-naphtho[1,2-*d*][1,3]dioxole-7,8-dicarbaldehyde (20)

Compound **19** (120 mg, 0.025 mmol) and $NaHCO_3$ (56 mg, 0.66 mmol) were dissolved in DMSO (10 ml) and the solution was heated to 100 °C. The reaction was kept at same temperature for 10 min. After cooled to room temperature, the reaction was quenched with cold brine (100 ml) and the aqueous mixture was extracted ether (50 ml × 2) and the combined organic layers was washed with saturated $NaHCO_3$ (25 ml) and brine (25 ml). The ether extract was then dried over $MgSO_4$ and concentrated. After column chromatography (hexane/CH_2Cl_2 = 1:3), pure **20** (53 mg, 60%) was isolated. ^{1}H NMR (400 MHz, $CDCl_3$) δ: 10.50 (s, 1H), 9.96 (s, 1H), 8.33 (s, 1H), 7.64 (d, J = 8.5, 1H), 7.34 (d, J = 8.5, 1H), 6.86 (d, J = 7.8 Hz, 1H), 6.83 (d, J = 1.4 Hz, 1H), 6.77 (dd, J = 1.6, 7.9 Hz, 1H), 6.08 (d, J = 1.1 Hz, 1H), 6.03 (d, J = 1.1 Hz, 1H), 5.93 (d, J = 1.2 Hz, 1H), 5.90 (d, J = 1.2 Hz, 1H) ^{13}C NMR (100 MHz, $CDCl_3$) δ: 193.6, 192.3, 147.9, 147.8, 147.2, 143.4, 142.4, 132.3, 131.4, 130.7, 129.9, 129.3, 125.3, 124.2, 120.5, 113.8, 110.8, 107.6, 101.9, 101.4. IR (CH_2Cl_2, cast): 1762, 1684, 1496, 1446, 1234, 1042, 925, 804 cm^{-1}. FAB-LRMS *m/z* (rel intensity): 349 ($[M+H]^+$, 25), 271 (22), 257 (13), 173 (12); FAB-HRMS Calcd for $C_{20}H_{13}O_6$ *m/z*: 349.0712 $[M+H]^+$, found 349.0714.

4.1.16. 9-Benzo[1,3]dioxol-5-yl-6-hydroxy-naphtho[1,2-*d*][1,3]dioxole-7,8-dicarbaxylic acid dimethyl ester (21)

A mixture of hydroxy acetal **1a** (1.5 g, 4.35 mmol), dimethyl acetylenedicarboxylate (625 mg, 4.39 mmol), acetic acid (0.62 ml), and dichloromethane (2 ml) was heated at 140 °C for 1 h. The mixture was cooled to room temperature, diluted with CH_2Cl_2 (30 ml), and washed with 5% $NaHCO_3$ solutions (3 × 30 ml). The organic solution was dried over $MgSO_4$ and concentrated. After column

chromatography (CH_2Cl_2), yellow solid **21** (940 mg, 51%) was isolated. ^{1}H NMR (300 MHz, $CDCl_3$) δ: 12.58 (s, 1H), 8.12 (d, J = 8.9 Hz, 1H), 7.18 (d, J = 8.8 Hz, 1H), 6.69–6.77 (m, 3H). 5.99 (dd, J = 1.3, 8.3 Hz, 2H), 5.83 (dd, J = 1.2, 6.3 Hz, 2H), 3.90 (s, 3H), 3.55 (s, 3H). ^{13}C NMR (100 MHz, $CDCl_3$) δ: 170.4, 168.8, 161.7, 148.6, 146.9, 146.5, 142.5, 131.2, 130.9, 124.5, 123.9, 121.6, 120.9, 119.6, 111.2, 110.6, 107.0, 101.6, 100.9, 100.1, 52.8, 51.9. IR (CH_2Cl_2, cast): 3489, 1735, 1684, 1492, 1444, 1246, 1037, 932, 812 cm^{-1}. FAB-LRMS m/z (rel intensity): 424 (M^+, 18), 393 (10), 392 (4), 371 (2), 178 (1). FAB-HRMS Calcd for $C_{22}H_{16}O_9$ m/z: 424.0794 $[M]^+$, found 424.0800.

4.1.17. 9-Benzo[1,3]dioxol-5-yl-6-hydroxy-naphtho[1,2-*d*][1,3]dioxole-7,8-dicarbaxylic acid-8-methyl ester (22)

To a solution of KOH (560 mg, 10 mmol) in MeOH (10 ml) was added **21** (20 mg, 0.047 mmol) and the mixture was refluxed for 2 h. After the completion of the reaction, 10% HCl (10 ml) was added to neutralize the reaction mixture before the mixture was extracted with CH_2Cl_2. The combined organic extracts was dried over $MgSO_4$ and concentrated. After column chromatography (CH_2Cl_2/MeOH = 20:1), pure **22** (11 mg 58%) was isolated as a white solid. ^{1}H NMR (400 MHz, $CDCl_3$) δ: 8.12 (d, J = 8.8 Hz, 1H), 7.19 (d, J = 8.8 Hz, 1H), 6.78 (s, 1H), 6.76 (d, J = 0.8 Hz, 2H), 6.00 (d, J = 1.3 Hz, 1H), 5.97 (d, J = 1.3 Hz, 1H), 5.83 (dd, J = 1.4, 8.4 Hz, 2H), 3.89 (s, 3H). ^{13}C NMR (100 MHz, $CDCl_3$) δ: 172.5, 168.9, 162.8, 151.8, 148.9, 146.9, 146.5, 142.6, 131.1, 124.6, 123.9, 121.9, 120.9, 119.9, 111.2, 110.6, 108.4, 107.1, 101.7, 100.9, 52.1. IR (CH_2Cl_2, film): 3439, 1734, 1564, 1380, 1225, 1034, 941, 805 cm^{-1}. FAB-LRMS m/z (rel intensity): 410 (M^+, 10), 393 (5), 377 (3), 338 (4), 176 (7). FAB-HRMS Calcd for $C_{21}H_{14}O_9$ m/z: 410.0638 $[M]^+$, found 410.0632.

4.1.18. 9-Benzo[1,3]dioxol-5-yl-6-methoxy-naphtho[1,2-*d*][1,3]dioxole-7,8-dicarbaxylic acid dimethyl ester (23)

To a solution of **21** (100 mg, 0.23 mmol) in DMF (5 ml) was added CH_3I (67 mg, 0.47 mmol) and K_2CO_3 (65 mg, 0.47 mmol). The mixture was stirred for 3 h at room temperature. After the completion of the reaction, the mixture was diluted with water and extracted with CH_2Cl_2. The organic fraction was dried over $MgSO_4$ and concentrated. After column chromatography (CH_2Cl_2), pure **23** (100 mg, 97%) was isolated. ^{1}H NMR (400 MHz, $CDCl_3$) δ: 7.85 (d, J = 8.8 Hz, 1H), 7.25 (d, J = 8.8 Hz, 1H), 6.76 (d, J = 8.1 Hz, 2H), 6.70 (dd, J = 1.42, 7.9 Hz, 1H), 5.99 (dd, J = 1.3, 9.6 Hz, 2H), 5.85 (dd, J = 1.3, 9.6 Hz, 2H), 4.03 (s, 3H), 3.90 (s, 3H), 3.55 (s, 3H). ^{13}C NMR (100 MHz, $CDCl_3$) δ: 168.2, 166.8, 155.9, 147.0, 146.9, 146.5, 142.9, 131.6, 131.4, 130.2, 124.7, 123.1, 121.1, 118.1, 117.7, 111.9, 110.7, 107.1, 101.6, 100.9, 63.8, 52.6, 52.2. IR (CH_2Cl_2, cast): 1735, 1624, 1492, 1440, 1368, 1218, 1038, 932, 812 cm^{-1}. FAB-LRMS m/z (rel intensity): 438 (M^+, 85), 407 (47), 377 (3), 349 (3). FAB-HRMS Calcd for $C_{23}H_{18}O_9$ m/z: 438.0951 $[M]^+$, found 438.0945.

4.1.19. 9-Benzo[1,3]dioxol-5-yl-6-methoxy-naphtho[1,2-*d*][1,3]dioxol-7,8-dicarbaxylic acid 8-methyl ester (24)

Compound **23** (90 mg, 0.20 mmol) was dissolved in hot MeOH (5 ml) and a hot MeOH solution of KOH (1.16 g, 20 mmol in 5 mL) was added. The mixture was stirred overnight at 65 °C. 10% HCl (75 ml) was then added and the product was extracted with CH_2Cl_2 (50 ml). The organic extract was dried over $MgSO_4$ and concentrated. After column chromatography (hexane/CH_2Cl_2 = 1:2), pure **24** (50 mg, 57%) was isolated as a white solid. ^{1}H NMR (300 MHz, $CDCl_3$) δ: 7.81 (d, J = 8.7 Hz, 1H), 7.30 (d, J = 8.9 Hz, 1H), 6.70–6.79 (m, 3H), 6.00 (dd, J = 1.2, 10.3 Hz, 2H), 5.88 (dd, J = 1.3, 8.2 Hz, 2H), 4.12 (s, 3H), 3.61 (s, 3H). ^{13}C NMR (100 MHz, $CDCl_3$) δ: 168.2, 167.6, 157.0, 147.7, 147.2, 146.6, 143.1, 132.4, 130.7, 123.8, 123.3, 121.8, 118.3, 115.1, 112.1, 110.7, 107.1, 101.8, 100.9, 64.4, 52.3. IR (CH_2Cl_2, cast): 3425, 1812, 1765, 1578, 1492, 1442, 1365, 1223, 1039, 929 cm^{-1}. FAB-LRMS m/z (rel intensity): 424 (M^+, 18), 393 (35), 391 (22), 338 (9), 176 (14). FAB-HRMS Calcd for m/z: $C_{22}H_{16}O_9$ m/z 424.0794 $[M]^+$, found 424.0784.

4.1.20. 10-(3-Benzyloxy-4-methoxy-phenyl)-furo[3′,4′:6,7]-naphtho[1,2-*d*][1,3]dioxol-7,9-dione (25)

As described previously in the synthesis of **3**,[21] acetal **1** (7 g, 36.05 mmol) was dissolved in dry THF (100 ml) under nitrogen and the solution was cooled to −78 °C. *n*-BuLi (2.5 M in hexanes, 14.4 ml, 34.84 mmol) was added over 5 min. The mixture was stirred for another 15 min, the addition of 3-benzyloxy-4-methoxybenzaldehyde (8.8 g, 36.32 mmol) in dry THF (20 ml) then followed. After stirred for 30 min, the solution was gradually warmed to room temperature and stirred for another 2.5 h. The reaction was quenched with water (100 ml) and the resulting mixture was extracted with ether (3 × 100 ml). The organic fraction was dried over $MgSO_4$ and concentrated to give crude hydroxyacetal **1a**. This crude hydroxy acetal was used in the following Diels–Alder reaction without further purified or characterized.

Mixture of hydroxy acetal **1a** (14.8 g, 33.90 mmol), maleic anhydride (3.32 g, 33.95 mmol), acetic anhydride (12.7 ml), and acetic acid (4.7 ml) was heated at 140 °C for 24 h. After this period, the reaction mixture was cooled to room temperature, diluted with CH_2Cl_2 (100 ml), and washed with 5% $NaHCO_3$ solution (3 × 100 ml). The organic fraction was dried over $MgSO_4$ and concentrated to furnish yellow solid anhydride **25** (8 g, 52%). This anhydride was used in the following reaction without further purification. ^{1}H NMR (400 MHz, $CDCl_3$) δ: 8.40 (s, 1H), 7.71 (d, J = 8.5 Hz, 1H), 7.26–7.41 (m, 6H), 6.93–6.98 (m, 2H), 6.90 (d, J = 1.2 Hz, 1H), 5.84 (d, J = 1.2 Hz, 1H), 5.67 (d, J = 1.1 Hz, 1H), 5.12 (AB, J = 12.3 Hz, 2H), 3.96 (s, 3H). ^{13}C NMR (100 MHz, $CDCl_3$) δ: 163.0, 161.6, 150.2, 148.5, 147.3, 144.7, 139.6, 137.2, 131.8, 128.4, 127.9, 127.8, 127.3, 126.5, 125.9, 123.2, 122.8, 122.6, 121.9, 115.6, 114.3, 110.7, 102.1, 71.2, 55.9. IR (CH_2Cl_2, cast): 1833, 1773, 1592, 1510, 1453, 1258, 1223, 1138, 900 cm^{-1}. FAB-LRMS m/z (rel intensity): 454 (M^+, 7), 443 (1), 388 (1), 371 (2), 329 (2). FAB-HRMS Calcd for $C_{27}H_{18}O_7$ m/z: 454.1053 $[M]^+$, found 454.1048.

4.1.21. 10-(4-Benzyloxy-3-methoxy-phenyl)-furo[3′,4′:6,7]-naphtho[1,2-*d*][1,3]dioxol-7,9-dione (26), 10-(3,4-bis-benzyloxy-phenyl)-furo[3′,4′:6,7]naphtho[1,2-*d*][1,3]dioxole-7,9-dione (27), 10-(3,4-dimethoxyphenyl)-furo[3′,4′:6,7]naphtho-[1,2-*d*][1,3]dioxole-7,9-dione (28) and 10-(4-trifluoromethoxyphenyl)-furo[3′,4′:6,7]naphtho[1,2-*d*][1,3]dioxole-7,9-dione (29)

Anhydrides **26–29** were synthesized as described for **25**. The acetal **1** was dissolved in dry THF under nitrogen and cooled to −78 °C. *n*-BuLi (2.5 M in hexanes) was added drop wise over 5 min. The mixture was stirred for another 15 min before the addition of appropriate aldehydes (4-benzyloxy-3-methoxybenzaldehyde for **26**, 3, 4-dibenzyloxy benzaldehyde for **27**, 3,4-dimethoxybenzaldehyde for **28**, 4-trifluoromethoxybenzaldehyde for **29**). After stirred for 30 min, the solution was gradually warmed to room temperature and was stirred for another 2.5 h. The reaction was quenched with water and the resulting mixture was extracted with ether. The ether extract was dried over $MgSO_4$ and concentrated to give corresponding hydroxyl acetals. The crude hydroxyl acetals were mixed with maleic anhydride, acetic anhydride, and acetic acid in CH_2Cl_2 and the mixture was heated to 140 °C for 24 h. After workup, 50% of **26** and 48% of **27** were obtained as yellow solids in pure form. Anhydrides **28** and **29** thus obtained were impure but used in the subsequent reaction without further purification or characterization. Compound **26**. ^{1}H NMR

(400 MHz, $CDCl_3$) δ: 8.41 (s, 1H), 7.73 (d, J = 8.6 Hz, 1H), 7.48 (d, J = 7.2 Hz, 2H), 7.29–7.44 (m, 4H), 6.97 (d, J = 8.1 Hz, 1H), 6.89 (s, 1H), 6.87 (d, J = 8.2 Hz, 1H), 5.92 (s, 2H), 5.21 (AB, J = 12.1 Hz, 2H), 3.85 (s, 3H). ^{13}C NMR (100 MHz, $CDCl_3$) δ: 163.0, 161.7, 148.8, 148.7, 148.6, 144.7, 139.7, 136.9, 131.92, 128.6, 128.0, 127.9, 127.5, 127.2, 126.0, 123.3, 122.9, 121.9, 114.3, 113.4, 112.8, 102.2, 71.0, 56.2; IR (CH_2Cl_2, cast) 1822, 1768, 1512, 1458, 1418, 1371, 1262, 1219, 1136, 898 cm^{-1}. EI-LRMS m/z (rel intensity): 454 (M^+, 100), 426 (<1), 422 (<1), 364 (16), 363 (51), 335 (6), 317 (3), 289 (4), 261 (5), 233 (4), 205 (3), 176 (3), 163 (5), 150 (2). EI-HRMS Calcd for $C_{27}H_{18}O_7$ m/z: 454.1053 $[M]^+$, found 454.1060. **27**. ^{1}H NMR (400 MHz, $CDCl_3$) δ: 8.40 (s, 1H), 7.71 (d, J = 8.5 Hz, 1H), 7.49 (d, J = 7.3 Hz, 2H), 7.26–7.44 (m, 9H), 7.02 (d, J = 8.2 Hz, 1H), 6.96 (d, J = 1.8 Hz, 1H), 6.91 (dd, J = 1.9, 8.1 Hz, 1H), 5.84 (s, 1H), 5.72 (s, 1H), 5.22 (d, J = 4.9 Hz, 2H), 5.12 (AB, J = 11.9 Hz, 2H). ^{13}C NMR (100 MHz, $CDCl_3$) δ: 163.0, 161.6, 149.6, 148.5, 148.0, 144.7, 139.6, 137.3, 137.1, 131.8, 128.5, 128.4, 128.0, 127.8, 127.8, 127.5, 127.4, 127.3, 125.9, 123.3, 122.8, 121.9, 116.7, 114.3, 113.6, 102.2, 71.5, 71.1. IR (CH_2Cl_2, cast): 1833, 1773, 1620, 1492, 1443, 1223, 1039, 900, 744 cm^{-1}. FAB-LRMS m/z (rel intensity): 529 (M^+, 9), 422 (1), 329 (3), 176 (4). FAB-HRMS Calcd for $C_{33}H_{22}O_7$ m/z: 530.1366 $[M]^+$, found 530.1364.

4.1.22. 10-(3-Benzyloxy-4-methoxy-phenyl)-9*H*-furo[3′,4':6,7]-naphtho[1,2-*d*][1,3]dioxol-7-one (30) and 10-(3-Benzyloxy-4-methoxy-phenyl)-7*H*-furo[3′,4′:6,7]naphtho[1,2-*d*][1,3]dioxol-9-one (31)

Anhydride **25** (200 mg, 0.44 mmol) and $NaBH_4$ (60 mg, 1.58 mmol) were dissolved in dry THF (10 ml) and the solution was stirred for 1 h at room temperature. After this period, 10% HCl was added cautiously to the reaction mixture and the reaction was stirred for another 30 min. The mixed solution was extracted with ether. The organic fraction was dried over $MgSO_4$ and concentrated. After column chromatography (hexane/CH_2Cl_2 = 1:2), pure **30** (120 mg, 63%) and **31** (30 mg, 16%) were isolated as yellow solids. Compound **30**. ^{1}H NMR (300 MHz, $CDCl_3$) δ: 8.33 (s, 1H), 7.64 (d, J = 8.5 Hz, 1H), 7.27–7.40 (m, 6H), 6.94 (d, J = 8.2 Hz, 1H), 6.86 (dd, J = 8.2, 1.8 Hz, 1H), 6.81 (d, J = 1.8 Hz, 1H), 5.83 (d, J = 1.0 Hz, 1H), 5.68 (d, J = 1.2 Hz, 1H), 5.16 (AB, J = 12.8 Hz, 2H), 4.90 (AB, J = 15.2 Hz, 2H), 3.96 (s, 3H). ^{13}C NMR (100 MHz, $CDCl_3$) δ: 171.1, 149.5, 147.2, 146.8, 145.8, 141.7, 139.7, 137.0, 130.7, 129.1, 128.6, 127.9, 127.1, 125.3, 121.9, 121.3, 121.1, 115.5, 111.7, 111.2, 101.4, 70.8, 69.4 55.9. IR (CH_2Cl_2, cast): 1758, 1627, 1510, 1457, 1258, 1134, 1070, 1021 cm^{-1}. FAB-LRMS m/z (rel intensity): 440 (M^+, 53), 439 (6), 413 (2), 350 (13). FAB-HRMS Calcd for $C_{27}H_{20}O_6$ m/z: 440.1260 $[M]^+$, found 440.1268. Anal. Calcd for $C_{27}H_{20}O_6$: C, 73.63; H, 4.58. Found: C, 73.02; H, 4.68. Compound **31**. ^{1}H NMR (300 MHz, $CDCl_3$) δ: 7.76 (s, 1H), 7.49 (d, J = 8.7 Hz, 1H), 7.41 (d, J = 6.8 Hz, 2H), 7.25–7.34 (m, 4H), 6.94 (d, J = 1.6 Hz, 2H), 6.92 (d, J = 1.3 Hz, 1H), 5.76 (d, J = 1.2 Hz, 1H), 5.60 (d, J = 1.2 Hz, 1H), 5.33 (s, 2H), 5.10 (AB, J = 12.2 Hz, 2H), 3.94 (s, 3H). ^{13}C NMR (100 MHz, $CDCl_3$) δ: 169.1, 149.5, 147.0, 144.9, 143.5, 138.1, 137.6, 137.4, 132.7, 128.3, 127.7, 127.6, 127.3, 122.8, 122.1, 120.7, 120.4, 120.0, 116.0, 113.5, 110.4, 101.3, 71.1, 67.70, 55.8. IR (CH_2Cl_2, cast): 1761, 1609, 1510, 1453, 1312, 1255, 1124, 1021, 755 cm^{-1}. FAB-LRMS m/z (rel intensity): 441 ($[M+H]^+$, 9), 440 (8), 391 (7), 350 (1). FAB-HRMS Calcd for $C_{27}H_{21}O_6$ m/z: 441.1338 $[M+H]^+$, found 441.1332.

4.1.23. 10-(3-Hydroxy-4-methoxy-phenyl)-9*H*-furo[3′,4′:6,7]-naphtho[1,2*d*][1,3]dioxol-7-one (32)

To a solution of **30** (20 mg, 0.045 mmol) in anhydrous CH_2Cl_2 (3 ml) at −78 °C was slowly added a solution of BBr_3 (1 M in CH_2Cl_2, 0.045 ml) and the mixture was stirred for 2 h at the same temperature. After this time, MeOH (2 ml) was added to the reaction mixture and the resulting solution was warmed back to room temperature and concentrated in vacuo. The residue was dissolved in ether (15 ml) and washed with saturated $NaHCO_3$ (10 ml), water (10 ml), and brine (10 ml). The organic extract was dried over $MgSO_4$ and concentrated. After column chromatography (hexane/CH_2Cl_2 = 1:2), pure **32** (11 mg, 73%) was isolated as a yellow solid. ^{1}H NMR (400 MHz, $CDCl_3$) δ: 8.39 (s, 1H), 7.67 (d, J = 8.7 Hz, 1H), 7.28 (d, J = 8.6 Hz, 1H), 6.89–6.91 (m, 2H), 6.80 (dd, J = 2.0, 8.2 Hz, 1H), 5.91 (dd, J = 1.4, 4.5 Hz, 2H), 5.69 (s, 1H), 5.17 (AB, J = 15.1 Hz, 2H), 3.95 (s, 3H). ^{13}C NMR (100 MHz, $CDCl_3$) δ: 171.2, 146.9, 146.3, 145.1, 141.8, 139.7, 130.8, 129.9, 129.2, 127.3, 125.4, 121.5, 121.1, 120.7, 115.5, 111.7, 110.0, 101.5, 69.6, 55.9. IR (CH_2Cl_2, cast): 3510, 1751, 1631, 1510, 1453, 1269, 1067, 1017, 804 cm^{-1}. FAB-LRMS m/z (rel intensity): 350 (M^+, 9), 338 (8), 326 (3), 279 (11), 255 (31), 253 (14), 239 (14), 219 (11), 185 (20), 173 (54), 149 (100), 113 (18). FAB-HRMS Calcd for $C_{20}H_{14}O_6$ m/z: 350.0790 $[M]^+$, found 350.0781. Anal. Calcd for $C_{27}H_{20}O_6$: C, 73.63; H, 4.58. Found: C, 73.02; H, 4.68.

4.1.24. 10-(4-Benzyloxy-3-methoxy-phenyl)-9*H*-furo[3′,4′:6,7]-naphtho[1,2-*d*][1,3]dioxol-7-one (33) and 10-(4-benzyloxy-3-methoxy-phenyl)-7*H*-furo[3′,4′:6,7]naphtho[1,2-*d*][1,3]dioxol-9-one (34)

Anhydride **26** (500 mg, 1.1 mmol) was reduced with $NaBH_4$ (130 mg, 3.43 mmol) in dry THF (20 ml) as described for **30**. After column chromatography (hexane/CH_2Cl_2 = 2:3), pure **33** (340 mg, 70%) and **34** (100 mg, 20%) were isolated as yellow solids. Compound **33**. ^{1}H NMR (400 MHz, $CDCl_3$) δ: 8.40 (s, 1H), 7.69 (d, J =8.7 Hz, 1H), 7.48 (d, J = 7.3 Hz, 2H), 7.28–7.40 (m, 4H), 6.95 (d, J = 8.0 Hz, 1H,), 6.85 (d, J = 1.8 Hz, 1H), 6.82 (dd, J = 1.9, 8.0 Hz, 1H), 5.90 (dd, J = 1.2, 5.0 Hz, 2H), 5.19 (AB, J = 15.2 Hz, 2H), 5.20 (s, 2H), 3.85 (s, 3H). ^{13}C NMR (100 MHz, $CDCl_3$) δ: 171.1, 148.9, 148.0, 146.8, 141.7, 139.6, 136.9, 130.7, 129.8, 129.2, 128.5, 127.9, 127.4, 127.2, 125.4, 121.4, 212.1, 113.1, 111.7, 101.5, 71.0, 69.6, 56.1. IR (CH_2Cl_2, cast): 1759, 1631, 1514, 1457, 1269, 1134, 1070, 1017, 737 cm^{-1}. FAB-LRMS m/z (rel intensity): 441 ($[M+H]^+$, 9), 440 (11), 439 (2), 371 (13), 349 (4), 257 (4). FAB-HRMS Calcd for $C_{27}H_{20}O_6$ m/z: 440.1260 $[M]^+$, found 440.1257. **34**. ^{1}H NMR (300 MHz, $CDCl_3$) δ: 7.78 (s, 1H), 7.48–7.52 (m, 3H), 7.30–7.7.39 (m, 4H), 6.96 (d, J = 8.2 Hz, 1H), 6.89 (d, J = 1.8 Hz, 1H), 6.85 (dd, J = 1.9, 8.1 Hz, 1H), 5.83 (s, 2H), 5.35 (d, J = 0.8 Hz, 2H), 5.20 (AB, J = 12.0 Hz, 2H), 3.83 (s, 3H). ^{13}C NMR (100 MHz, $CDCl_3$) δ: 169.2, 148.4, 148.2, 145.0, 143.6, 138.2, 137.6, 137.3, 132.8, 128.5, 128.4, 127.8, 127.5, 122.2, 122.2, 120.8, 120.7, 120.2, 113.9, 113.6, 112.5, 101.4, 71.0, 67.8, 56.1. IR (CH_2Cl_2, cast): 1762, 1609, 1510, 1453, 1414, 1312, 1124, 1021 cm^{-1}. FAB-LRMS m/z (rel intensity): 441 ($[M+H]^+$, 11), 440 (12), 439 (3), 391 (4), 349 (4), 341 (<1). FAB-HRMS Calcd for $C_{27}H_{20}O_6$ m/z: 440.1260 $[M]^+$, found 440.1253.

4.1.25. 10-(4-Hydroxy-3-methoxy-phenyl)-9*H*-furo[3′,4′:6,7]-naphtho[1,2-*d*][1,3]dioxol-7-one (35)

To a solution of **33** (50 mg, 0.11 mmol) in anhydrous CH_2Cl_2 (5 ml) at −78 °C was slowly added a solution of BBr_3 (1 M in CH_2Cl_2, 0.12 ml). The reaction mixture was allowed to proceed as described for **32**. After column chromatography (hexane/CH_2Cl_2 = 1:2), pure **35** (28 mg, 72%) was isolated as a yellow solid. ^{1}H NMR (400 MHz, $CDCl_3$) δ: 8.40 (s, 1H), 7.69 (d, J = 8.6 Hz, 1H), 7.29 (d, J = 8.6 Hz, 1H), 6.97 (d, J = 8.3 Hz, 1H), 6.84 (dd, J = 1.8, 8.0 Hz, 1H), 6.81 (d, J = 1.7 Hz, 1H), 5.91 (dd, J = 1.2, 6.6 Hz, 2H), 5.72 (s, 1H), 5.19 (AB, J = 15.1 Hz, 2H), 3.86 (s, 3H). ^{13}C NMR (100 MHz, $CDCl_3$) δ: 171.2, 146.9, 146.1, 145.5, 141.8, 139.7, 130.8, 129.4, 128.7, 127.3, 125.5, 121.9, 121.6, 121.1, 114.0, 111.9, 111.8, 101.5, 69.6, 56.0. IR (CH_2Cl_2, cast): 3446, 1756, 1631, 1514, 1460, 1265, 1074, 1017 cm^{-1}. FAB-LRMS m/z (rel intensity): 350 (M^+, 24), 326 (13), 281 (39), 255 (32), 221 (88),

207 (56), 173 (100), 147 (75), 109 (94). FAB-HRMS Calcd for $C_{20}H_{14}O_6$ *m/z*: 350.0790 $[M]^+$, found 350.0783.

4.1.26. 10-(3,4-Bis-benzyloxy-phenyl)-9*H*-furo[3′,4′:6,7]naphtho[1,2-*d*][1,3]dioxol-7-one (36) and 10-(3,4-Bis-benzyloxy-phenyl)-7*H*-furo[3′,4′:6,7]naphtho[1,2-*d*][1,3]dioxol-9-one (37)

Anhydride **27** (1 g, 1.88 mmol) was reduced with $NaBH_4$ (24 mg, 6.35 mmol) in dry THF (20 ml) as described for **30** and **31**. After column chromatography (hexane/CH_2Cl_2 = 3:1), pure **36** (610 mg, 63%) and **37** (140 mg, 14%) were isolated as yellow solids. Compound **36**. ^1H NMR (400 MHz, $CDCl_3$) δ: 8.33 (s, 1H), 7.63 (d, J = 8.5 Hz, 1H), 7.50 (d, J = 7.0 Hz, 2H), 7.26–7.40 (m, 9H), 7.00 (d, J = 8.0 Hz, 1H), 6.87 (s, 1H), 6.83 (d, J = 7.8 Hz, 1H), 5.81 (s, 1H), 5.71 (s, 1H), 5.22 (s, 2H), 5.17 (AB, J = 12.6 Hz, 2H), 4.93 (AB, J = 15.2 Hz, 2H). ^{13}C NMR (100 MHz, $CDCl_3$) δ: 171.1, 148.9, 147.9, 146.8, 141.7, 139.7, 137.2, 130.7, 129.9, 129.1, 128.5, 127.9, 127.6, 127.4, 127.2, 125.4, 122.2, 121.4, 121.1, 116.4, 114.1, 111.7, 101.4, 71.2, 71.1, 69.4. IR (CH_2Cl_2, cast): 1760, 1627, 1509, 1458, 1266, 1129, 1070, 1015, 739 cm^{-1}. FAB-LRMS *m/z* (rel intensity): 516 (M^+, 39), 515 (5), 460 (<1), 426 (9), 391 (7), 371 (2), 335 (5), 181 (7). FAB-HRMS Calcd for $C_{33}H_{24}O_6$ *m/z*: 516.1573 $[M]^+$, found 516.1575. **37**. ^1H NMR (500 MHz, $CDCl_3$) δ: 7.77 (s, 1H), 7.50–7.48 (m, 3H), 7.41 (d, J = 7.2 Hz, 2H), 7.29–7.36 (m, 7H), 7.01 (d, J = 8.2 Hz, 1H), 6.97 (d, J = 1.8 Hz, 1H), 6.90 (dd, J = 1.8, 8.2 Hz, 1H), 5.76 (s, 1H), 5.66 (s, 1H), 5.35 (s, 2H), 5.20 (AB, J = 11.8 Hz, 2H), 5.11 (AB, J = 12.2 Hz, 2H). ^{13}C NMR (100 MHz, $CDCl_3$) δ: 169.1, 149.0, 147.8, 144.9, 143.5, 137.9, 137.5, 137.4, 132.7, 128.6, 128.3, 128.2, 127.8, 127.6, 127.5, 127.4, 127.3, 123.1, 122.2, 120.7, 120.0, 117.2, 113.5, 113.4, 101.3, 71.5, 71.1, 67.7. IR (CH_2Cl_2, cast): 1759, 1609, 1505, 1455, 1312, 1208, 1122, 1018, 735 cm^{-1}. FAB-LRMS *m/z* (rel intensity): 516 (M^+, 69), 515 (9), 426 (8), 425 (6), 371 (6), 369 (5), 181 (9). FAB-HRMS Calcd for $C_{33}H_{24}O_6$ *m/z*: 516.1573 $[M]^+$, found 516.1575.

4.1.27. 10-(3,4-Dihydroxy-phenyl)-9*H*-furo[3′,4′:6,7]naphtho-[1,2-*d*][1,3]dioxol-7-one (38)

To a solution of **36** (50 mg, 0.096 mmol) in anhydrous CH_2Cl_2 (5 ml) at −78 °C was added slowly a solution of BBr_3 (1 M in CH_2Cl_2, 0.22 ml) and the reaction was allowed to proceed as described for **32**. After column chromatography (CH_2Cl_2/methanol = 19:1), pure **36** (24 mg, 77%) was isolated. ^1H NMR (300 MHz, CD_3COCD_3) δ: 8.42 (s, 1H), 7.88 (d, J = 8.6 Hz, 1H), 7.41 (d, J = 8.6 Hz, 1H), 6.91 (d, J = 2.2 Hz, 1H), 6.89 (s, 1H), 6.77 (dd, J = 2.1, 8.0 Hz, 1H), 5.97 (d, J = 3.6 Hz, 2H), 5.61 (s, 2H), 5.24 (AB, J = 15.0 Hz, 2H). ^{13}C NMR (100 MHz, CD_3COCD_3) δ: 171.0, 147.4, 145.7, 145.2, 142.5, 140.7, 131.7, 130.5, 129.2, 126.9, 126.1, 122.1, 122.0, 121.5, 117.1, 115.4, 112.2, 102.1, 69.9. IR (CH_2Cl_2, cast): 3354, 1737, 1624, 1510, 1453, 1269, 1070, 1017, 804 cm^{-1}. FAB-LRMS *m/z* (rel intensity): 336 (M^+, 7), 176 (2). FAB-HRMS Calcd for $C_{19}H_{12}O_6$ *m/z*: 336.0634 $[M]^+$, found 336.0628.

4.1.28. 10-(3,4-Dimethoxy-phenyl)-9*H*-furo[3′,4′:6,7]naphtho-[1,2-*d*][1,3]dioxol-7-one (39)

Anhydride **28** (1 g, 2.64 mmol) was reduced with $NaBH_4$ (350 mg, 9.24 mmol) in dry THF (20 ml) as described for **30**. After column chromatography (hexane/CH_2Cl_2 = 3:1), pure **39** (630 mg, 65%) was isolated. ^1H NMR (400 MHz, $CDCl_3$) δ: 8.41 (s, 1H), 7.69 (d, J = 8.6 Hz, 1H), 7.30 (d, J = 8.6 Hz, 1H), 6.90–6.92 (m, 2H), 6.83 (d, J = 1.8 Hz, 1H), 5.91 (d, J = 0.6 Hz, 2H), 5.20 (AB, J = 15.1 Hz, 2H), 3.95 (s, 3H), 3.85 (s, 3H). ^{13}C NMR (100 MHz, $CDCl_3$) δ: 170.9, 148.8, 148.4, 146.8, 141.6, 139.6, 130.7, 129.2, 127.8, 127.7, 127.1, 125.3, 121.4, 121.1, 121.0, 112.7, 111.6, 110.6, 101.4, 69.4, 55.9, 55.8. IR (CH_2Cl_2, cast): 1758, 1627, 1514, 1457, 1258, 1134, 1070, 1024 cm^{-1}. FAB-LRMS *m/z* (rel intensity): 364 (M^+, 39), 326 (10), 281 (12), 243 (13), 191(18), 109 (100). FAB-HRMS Calcd for $C_{21}H_{16}H_6$ *m/z*: 364.0947 $[M]^+$, found 364.0942.

4.1.29. 10-(4-Trifluoromethoxy-phenyl)-9*H*-furo[3′,4′:6,7]-naphtho[1,2-*d*][1,3]dioxol-7-one (40)

Anhydride **29** (1 g, 2.48 mmol) was reduced with $NaBH_4$ (330 mg, 8.70 mmol) in dry THF (20 ml) as described for **30**. After column chromatography (hexane/CH_2Cl_2 = 3:2), pure **40** (610 mg, 63%) was isolated as a yellow solid. ^1H NMR (400 MHz, $CDCl_3$) δ: 8.44 (s, 1H), 7.71 (d, J = 8.6 Hz, 1H), 7.37 (d, J = 8.7 Hz, 2H), 7.25–7.32 (m, 3H), 5.89 (s, 2H), 5.16 (s, 2H). ^{13}C NMR (100 MHz, $CDCl_3$) δ: 170.8, 149.1, 148.1, 147.1, 141.6, 139.6, 135.4, 130.7, 130.5, 127.9, 125.6, 121.1, 120.3, 111.9, 101.6, 69.3. IR (CH_2Cl_2, cast): 1765, 1631, 1458, 1259, 1215, 1677, 1071, 1020 cm^{-1}. FAB-LRMS *m/z* (rel intensity): 387 (M^+, 100), 386 (11), 359 (6), 315 (5), 299 (3), 289 (2), 189 (3), 176 (3). FAB-HRMS Calcd for $C_{20}H_{11}O_5F_3$ *m/z*: 388.0559 $[M]^+$, found 388.0558.

5. Materials and methods for cell culture

5.1. Reagents

Hepatitis B surface antigen (HBsAg) and e antigen (HBeAg) enzyme immunoassay (EIA) kits were purchased from Bio-Rad (Hercules, CA, USA). Fetal calf serum was obtained from Hyclone (Logan, UT, USA). Dulbecco's modified Eagle's medium (DMEM) was obtained from Gibco/BRL (Gaithersbung, MD, USA). [α-^{32}P] dCTP was obtained from PerkinElmer Life Sciences (MA, USA). Sea Kem LE-agarose was purchased from FMC Bioproducts (Rockland, MA, USA).

5.2. Cell culture

Human hepatoblastoma HepA2 cell line is derived from HepG2 cells by transfecting with two tandem repeats of the HBV genome and continually secretes HBsAg and HBeAg into the culture medium.[28] The 1.3ES2 cell line is a clonal derivative of HepG2 cells in which the 1.3-copies of the entire HBV genome was stably integrated in the host genome.[26] These cell lines were used to assess the antiviral activity of helioxanthin and its analogues. The lamivudine-resistant cell line M33 is also a hepatoblastoma HepG2 cell line stably transfected with 1.3-copies of entire HBV genome, which contains the L515M/M539V double mutation.[29] This stable cell line secretes lamivudine-resistant HBV particles containing viral DNA and DNA polymerase activity. Stock cultures of human hepatoma cells HepA2, 1.3ES2 and M33 were maintained in DMEM supplemented with 10% fetal calf serum and antibiotics (100 IU/ml each of penicillin and streptomycin) in a humidified atmosphere containing 5% CO_2 and 95% air at 37 °C. The cultures were passaged by trypsinization every 4 days. For bioassays, cells were plated either in 24-well plates at a density of 8×10^4 cells/well or in 100-mm culture dishes at a density of 1.5×10^6 cells/dish in DMEM medium containing 10% fetal calf serum.

5.3. Quantification of HBsAg and HBeAg

Cells were seeded either in 96-well plates at a density of 3×10^4 cells/well or in 24-well plates at a density of 8×10^4 cells/well in DMEM medium containing 10% fetal calf serum. After 24 h of incubation, the cells were washed twice with phosphate-buffered saline (PBS), pH 7.0, and treated with various concentrations of drugs in serum-free DMEM for 48 h. The HBsAg and HBeAg in the culture medium were measured by the appropriate enzyme immunoassay (EIA) kits (Bio-Rad, CA, USA). The viability of cells was determined by a WST-1 cell proliferation assay. For the WST-1 assay, WST-1 (Roche Diagnostics, Mannheim, Germany) was added to each well and incubated for 0.5 h. The amount of formazan dye formed can be correlated to the number of

metabolically active cells and is quantitatively determined using a scanning multi-well spectrophotometer (ELISA reader) at absorbance 450 nm.

5.4. Quantitative detection of HBV DNA by real-time light cycler PCR

We have used dilutions of known amounts of HBV-DNA from plasmid as a control. The standard curve showed a good linear range when 10^3–10^7 copies of plasmid DNA were used as templates (data not shown). Cells were seeded in 100 mm culture dishes at a density of 5×10^6 cells/well, then treated with various concentrations of drug in serum-free DMEM for 72 h. For quantification of HBV DNA, viral DNA was extracted from culture media using High Pure Viral Nucleic Acid Kit (Roche, Mannheim, Germany) according to the manufacturer's instructions. The PCR primers used were purchased from Tib-Molbiol (Berlin, Germany). The oligonucleotide sequences of primers were: HBV Forward: 5′-CA GGTCTGTGCCAAG-3′ (the accession number of GenBank: V01460, nt 1168–1182) HBV Reverse: 5′-TGCGGGATAGGACAA-3′ (nt 1359–1345). The PCR cycling program consisted of an initial denaturing step at 95 °C for 10 min, followed by 45 amplification cycles at 95 °C for 12 s, 54 °C for 20 s.

5.5. RNA isolation and Northern blot analysis

Total RNA was extracted from the cells using the phenol and guanidium isothiocyanate method.[30] The RNA (20 μg) was denatured by 2.2 M formaldehyde, separated on a denaturing formaldehyde 1.2% agarose gel, and transferred to a nylon membrane (Hybond-XL, Amersham). The membrane was hybridized with a ^{32}P-radiolabelled full-length HBV probe. The relative amount of total RNA applied was normalized to that of glyceraldehyde-3-phosphate dehydrogenase.

5.6. Transient transfections and luciferase assay

HepA2 cells were transfected with various plasmids by using lipofectamine 2000 transfection reagent (Invitrogen). The transfected cells were changed to a serum-free DMEM with drug for two days. To prepare total cell lysate from transfected cells for luciferase activity measurements, medium was aspirated from the cell culture and the cells were gently rinsed with PBS. Cells were scrapped from the plates and collected through centrifugation. The supernatant was collected for protein and luciferase activity measurements immediately following lysate preparation. Protein concentrations of the resultant cell lysates were measured by the Bradford method. Lysates prepared from transfected cells were analyzed for luciferase activity using a luminometer and the Promega Luciferase Assay System as described by the manufacturer (Promega). Luciferase activities were normalized to the amount of protein in each lysate. For all transient transfections with promoter-luciferase reporter constructs, the level of luciferase activity was determined without drug treatment to be set to one. The transfection efficiency was normalized using the activity of β-galactosidase as an internal control. The values are means plus and minus the standard error of the mean of at least three independent experiments.

5.7. Plasmids

The plasmids were constructed by standard DNA cloning procedures and polymerase chain reaction (PCR) methods.[31] The HBV sequence used in this study is of *ayw* subtype.[32] The accession number of GeneBank: V01460, Eco RI site as nucleotide 1. To generate pXP-Luc, the *Xbal-HindIII* fragments containing the X promoter from pXP-CAT were inserted into the *MluI-HindIII* site of the pGL3-Basic vector (Promega, Madison, WI). The pS1P-Luc, pS2P-Luc, pCP-Luc, pE/XP-Luc plasmids were generous gifts from Dr. Chungming Chang (National Health Research Institutes, Taiwan).

Acknowledgments

The authors thank Drs. Kak-Shan Shia and Shu-Jen Chen for the advice and comments on the manuscript; Dr. Chungming Chang for providing pS1P-Luc, pS2P-Luc, pCP-Luc, pE/XP-Luc plasmids. This work was supported by grants: NSC 97-3112-B-010-003 from National Science Council and Ministry of Education, Aim for the Top University Plan, Republic of China.

Supplementary data

Supplementary data associated with this article can be found, in the online version, at doi:10.1016/j.bmc.2009.12.038.

References and notes

1. Chang, M. H.; Chen, C. J.; Lai, M. S.; Hsu, H. M.; Wu, T. C.; Kong, M. S.; Liang, D. C.; Shau, W. Y.; Chen, D. S. *N. Eng. J. Med.* **1997**, *336*, 1855.
2. Robinson, W. S. *Annu. Rev. Microbiol.* **1977**, *31*, 357.
3. Yuh, C. H.; Ting, L. P. *J. Virol.* **1990**, *64*, 4281.
4. Dienstag, J. L.; Perrillo, R. P.; Schiff, E. R.; Bartholomew, M.; Vicary, C.; Rubin, M. *N. Eng. J. Med.* **1995**, *333*, 1657.
5. Walsh, K. M.; Woodall, T.; Lamy, P.; Wight, D. G.; Bloor, S.; Alexander, G. J. *Gut* **2001**, *49*, 436.
6. Franco, J.; Saeian, K. *J. Vasc. Interv. Radiol.* **2002**, *13*, S191.
7. Langley, D. R.; Walsh, A. W.; Baldick, C. J.; Eggers, B. J.; Rose, R. E.; Levine, S. M.; Kapur, A. J.; Colonno, R. J.; Tenney, D. J. *J. Virol.* **2007**, *81*, 3992.
8. Ruiz-Sancho, A.; Sheldon, J.; Soriano, V. *Expert Opin. Biol. Ther.* **2007**, *7*, 751.
9. Lee, H. S.; Chung, Y. H.; Lee, K. S.; Byun, K. S.; Paik, S. W.; Han, J. Y.; Yoo, K.; Yoo, H. W.; Lee, J. H.; Yoo, B. C. *Hepatology* **2006**, *43*, 982.
10. Zoulim, F. *J. Clin. Virol.* **2001**, *21*, 243.
11. Yeh, C. T.; Chien, R. N.; Chu, C. M.; Liaw, Y. F. *Hepatology* **2000**, *31*, 1318.
12. Locarnini, S.; Mason, W. S. *J. Hepatol.* **2006**, *44*, 422.
13. Mohanty, S. R.; Kupfer, S. S.; Khiani, V. *Nat. Clin. Pract. Gastroenterol. Hepatol.* **2006**, *3*, 446.
14. Lee, Y. S.; Suh, D. J.; Lim, Y. S.; Jung, S. W.; Kim, K. M.; Lee, H. C.; Chung, Y. H.; Yoo, W.; Kim, S. O. *Hepatology* **2006**, *43*, 1385.
15. Deres, K.; Schroder, C. H.; Paessens, A.; Goldmann, S.; Hacker, H. J.; Weber, O.; Kramer, T.; Niewohner, U.; Pleiss, U.; Stoltefuss, J.; Graef, E.; Koletzki, D.; Masantschek, R. N.; Reimann, A.; Jaeger, R.; Gross, R.; Beckermann, B.; Schlemmer, K. H.; Haebich, D.; Rubsamen-Waigmann, H. *Science* **2003**, *299*, 893.
16. Tan, T. M.; Chen, Y.; Kong, K. H.; Bai, J.; Li, Y.; Lim, S. G.; Ang, T. H.; Lam, Y. *Antiviral Res.* **2006**, *71*, 7.
17. Tseng, Y. P.; Kuo, Y. H.; Hu, C. P.; Jeng, K. S.; Janmanchi, D.; Lin, C. H.; Chou, C. K.; Yeh, S. F. *Antiviral Res.* **2008**, *77*, 206.
18. Li, Y.; Fu, L.; Yeo, H.; Zhu, J. L.; Chou, C. K.; Kou, Y. H.; Yeh, S. F.; Gullen, E.; Austin, D.; Cheng, Y. C. *Antiviral Chem. Chemother.* **2005**, *16*, 193.
19. Mizufune, H.; Nakamura, M.; Mitsudera, H. *Tetrahedron Lett.* **2001**, *42*, 437.
20. Holmes, T. L.; Stevenso, R. *J. Chem. Soc. C-Org.* **1971**, 2091.
21. Stevenson, R.; Weber, J. V. *J. Nat. Prod.* **1989**, *52*, 367.
22. Charlton, J. L.; Oleschuk, C. J.; Chee, G. L. *J. Org. Chem.* **1996**, *61*, 3452.
23. Yeo, H.; Li, Y.; Fu, L.; Zhu, J. L.; Gullen, E. A.; Dutschman, G. E.; Lee, Y.; Chung, R.; Huang, E. S.; Austin, D. J.; Cheng, Y. C. *J. Med. Chem.* **2005**, *48*, 534.
24. Cow, C.; Leung, C.; Charlton, J. L. *Can. J. Chem.-Revue Canadienne De Chim.* **2000**, *78*, 553.
25. Yeh, S. F.; Hong, C. Y.; Huang, Y. L.; Liu, T. Y.; Choo, K. B.; Chou, C. K. *Antiviral Res.* **1993**, *20*, 185.
26. Chou, Y. C.; Jeng, K. S.; Chen, M. L.; Liu, H. H.; Liu, T. L.; Chen, Y. L.; Liu, Y. C.; Hu, C. P.; Chang, C. *J. Virol.* **2005**, *79*, 1813.
27. Ying, C.; Li, Y.; Leung, C. H.; Robek, M. D.; Cheng, Y. C. *Proc. Natl. Acad. Sci. U.S.A.* **2007**, *104*, 8526.
28. Chang, C. M.; Jeng, K. S.; Hu, C. P.; Lo, S. J.; Su, T. S.; Ting, L. P.; Chou, C. K.; Han, S. H.; Pfaff, E.; Salfeld, J., et al *EMBO J.* **1987**, *6*, 675.
29. Huang, R. L.; Huang, Q.; Chen, C. F.; Chang, T. T.; Chou, C. J. *Chin. Pharm. J.* **2003**, *55*, 371.
30. Gruffat, D.; Piot, C.; Durand, D.; Bauchart, D. *Anal. Biochem.* **1996**, *242*, 77.
31. Mullis, K.; Faloona, F.; Scharf, S.; Saiki, R.; Horn, G.; Erlich, H. *Cold Spring Harb. Symp. Quant. Biol.* **1986**, *51*, 263.
32. Galibert, F.; Mandart, E.; Fitoussi, F.; Tiollais, P.; Charnay, P. *Nature* **1979**, *281*, 646.